Policy Research Working Paper 9845

Urban CO_2 Emissions

A Global Analysis with New Satellite Data

Susmita Dasgupta
Somik Lall
David Wheeler

WORLD BANK GROUP
Urban, Disaster Risk Management, Resilience and Land Global Practice
November 2021

Policy Research Working Paper 9845

Abstract

This paper estimates an urban carbon dioxide emissions model using satellite-measured carbon dioxide concentrations from 2014 to 2020, for 1,236 cities in 138 countries. The model incorporates the global trend in carbon dioxide concentration, seasonal fluctuations by hemisphere, and a large set of georeferenced variables that incorporate carbon dioxide–intensive industry structure, emissions from agricultural and forest fires in neighboring areas, demography, the component of income that is uncorrelated with industry structure, and relevant geographic conditions. The income results provide the first test of an Environmental Kuznets Curve relationship for carbon dioxide based on actual observations. They suggest an environmental Kuznets curve that reaches a peak near or above $40,000 per capita, which is at the 90th percentile internationally. The research also finds that economic development has a significant effect on the direction of the relationship between population density and carbon dioxide emissions. The relationship is positive at very low incomes but becomes negative at higher incomes. The paper also uses cities' mean regression residuals to index their carbon dioxide emissions performance within and across regions, decomposes model carbon dioxide predictions into broad source categories for each city, and uses the regression residuals to explore the impact of subway systems. The findings show significantly lower carbon dioxide emissions for subway cities.

This paper is a product of the Urban, Disaster Risk Management, Resilience and Land Global Practice. It is part of a larger effort by the World Bank to provide open access to its research and make a contribution to development policy discussions around the world. Policy Research Working Papers are also posted on the Web at http://www.worldbank.org/prwp. The authors may be contacted at sdasgupta@worldbank.org, slall1@worldbank.org, and wheelrdr@gmail.com.

Urban CO_2 Emissions: A Global Analysis with New Satellite Data

Susmita Dasgupta*
Somik Lall
David Wheeler

World Bank

Keywords: CO2 emissions, Environment Kuznets Curve, City CO2 performance metrics
JEL classification: Q54; Q58; R40; R11

Acknowledgments: The authors thank Richard Damania, Sam Fankhauser, Stephane Hallegatte, Matt Kahn, Joanna Masic, Rick Van der Ploeg, Tony Venables, Sameh Wahba, and seminar participants at the World Bank and FCDO for helpful discussions. The authors acknowledge the generous financial support from the UK FCDO. The findings, interpretations, and conclusions expressed in this paper are entirely those of the authors. They do not necessarily represent the views of the International Bank for Reconstruction and Development/World Bank and its affiliated organizations, or those of the Executive Directors of the World Bank or the governments they represent.

* Authors' names in alphabetical order.

Summary

This paper estimates an urban CO2 emissions model using satellite-measured CO2 concentrations from 2014 to 2020, for 1,236 cities in 138 countries. The model incorporates the global trend in CO2 concentration, seasonal fluctuations by hemisphere, and a large set of georeferenced variables that incorporate CO2-intensive industry structure, emissions from agricultural and forest fires in neighboring areas, demography, the component of income that is uncorrelated with industry structure, and relevant geographic conditions. The income results provide the first test of an Environmental Kuznets Curve relationship for CO2 based on actual observations. We find evidence for an EKC that reaches a peak near or above $40,000 per capita, which is at the 90th percentile internationally. We also find that economic development has a significant effect on the direction of the relationship between population density and CO2 emissions. The relationship is positive at very low incomes, but becomes negative at higher incomes.

We explore other implications of our estimates in a series of exercises. Using cities' mean regression residuals to index their CO2 emissions performance, we find wide variation within and across regions. Overall performance exceeds model-based expectations in India, Western Europe and the former Comecon countries, while it falls short in China, the rest of East Asia & Pacific, Middle East & North Africa and Sub-Saharan Africa. We also decompose model CO2 predictions into five broad source categories for each city. We find particularly important roles for CO2-intensive industry structure in India, China and other East Asia & Pacific countries; agricultural and forest-clearing fires in Sub-Saharan Africa; the component of income per capita that is uncorrelated with industry structure in Latin America & Caribbean, North America and Western Europe; population and population density in Sub-Saharan Africa, India and other South Asian countries; and climate in the former Comecon countries.

Our results can also inform the discussion of policy instruments for CO2 emissions reduction. Many policy analysts who support Pigouvian pricing also argue for a non-Pigouvian supplement: coordinated public investment in low-carbon land development, energy and transport that will accelerate the transition to low-carbon economies. We explore the non-Pigouvian proposition for subway investments, drawing on a recent global survey of subway systems. We divide our 1,236 regression residuals into deciles, with the largest negative residuals in the first decile, and identify the subset of 132 global subway cities in each decile. We find that subway cities are four times more numerous among first-decile cities than among tenth-decile cities. We also find that representation of subway cities declines steadily across deciles. While these results provide strong suggestive support for the non-Pigouvian view, they are subject to potential endogeneity that should be considered in future research.

This research is only one of many potential applications for our global CO2 database, which covers all terrestrial areas at 10 km resolution. The same CO2 emissions model could be used to track progress for large and small cities within subregions or countries, subregions within countries, or project areas.

1. Introduction

The World Meteorological Organization forecasts that the current greenhouse gas (GHG) emissions trend will increase global temperature by 3-5 degrees C by 2100 (Reuters 2018). This would far overshoot the 2-degree limit pledged by the 2015 Paris climate accord (COP 21) and might have a catastrophic impact (Steffen et al. 2018; World Bank 2012). In response, several industrial nations pledged very steep emissions reductions at the recent Leaders' Summit on Climate (April 22-23, 2021).

On April 2, 2021, the President of the World Bank responded with a new Climate Change Action Plan (World Bank 2021) that expands participation in large-scale climate finance and commits the World Bank to align all new World Bank operations with the objectives of the Paris Agreement by July 1, 2023. IFC and MIGA will align 85% of new operations by July 1, 2023 and 100% by July 1, 2025. The announcement highlights the need for new metrics to achieve impact by measuring GHG emissions reductions. In this context, this paper makes four contributions to the knowledge base on GHG emissions and underlying drivers.

First, the Climate Change Action Plan confronts a striking information shortfall at the outset: near-total absence of directly-measured local and regional GHG data for problem diagnosis, program design and performance assessment. In the global arena, consistently-measured GHG estimates are only available for about 80 urban areas, and over half of those are in developed countries (C40 2021). In addition, few of the available estimates incorporate actual GHG emissions. Most rely on emissions parameters from engineering studies, which are applied to survey-based activity measures for transport, energy production and manufacturing. Standard engineering estimates are particularly suspect for developing countries, because many of the parameters have been calibrated using databases and models developed for high-income economies.

Recently, the advent of satellite-based GHG measurement has greatly expanded the potential for empirical assessment. High-resolution observations of atmospheric GHG concentrations are now available from several platforms, including NASA's OCO-2 and OCO-3 instruments, the European Space Agency's METOP-A and TROPOMI (Sentinel-5P) platforms, and the Japan Space Exploration Agency's GOSAT and GOSAT-2. Detailed technical assessments of measures from these platforms have verified that they provide useful and comprehensive information for global carbon emissions analysis (Pan et al. 2021; Wu et al. 2020; Labzovskii et al. 2019). Along with research verification, the first global satellite-based GHG studies have begun to emerge for small samples of cities (e.g., Wu et al. 2020).

In this paper, we extend the domain for analysis with a panel of satellite-measured CO2 concentrations for 1,236 urban areas with populations greater than 500,000. The database covers the period 2014-2020 and includes cities in 138 countries in Africa (41), the Americas (22), Asia (44), Europe (29) and Oceania (2).

Second, we provide the first test of an Environmental Kuznets Curve (EKC) relationship for CO2 based on actual observations. We specify an econometric model of cities' atmospheric CO2 concentrations that incorporates a large set of georeferenced determinants. We find evidence for an EKC that reaches a peak near or above $40,000 per capita, which is at the 90th percentile internationally. We also explore the relationship between population density and urban CO2 emissions at different levels of economic development.

Third, we use the results to estimate the expected CO2 concentration for each city, given its geographic, demographic and economic characteristics. We explore the implications using regression residuals as performance indicators that identify cities whose CO2 emissions are less than or greater than model-based expectations. This provides the first empirical scorecard of city performance in CO2 emissions management.

Fourth, we use the econometric results to address a critical policy question on the role of public investment as a supplement to Pigouvian policy in mitigating CO2 emissions. Economists generally support emissions reduction via emissions taxation or permit trading (Stiglitz and Stern 2021; Jacobs and van der Ploeg 2019; King et al. 2019; Klenert et al. 2018). Many policy analysts who support Pigouvian pricing also argue for a non-Pigouvian supplement: coordinated public investment in low-carbon land development, energy and transport that will accelerate the transition to low-carbon economies (van der Ploeg and Venables 2020). Investments in subway systems provide an interesting test case for the non-Pigouvian approach. Reduced motor vehicle emissions and energy efficiencies associated with higher-density development are frequently cited as carbon-saving advantages of mass transit systems. By implication, cities with subways should have followed lower-carbon development paths, other things equal. We explore this proposition with our regression residuals, drawing on a recent global survey of subway systems (Turner and Gonzalez-Navarro 2018).

The remainder of the paper is organized as follows. Section 2 introduces the econometric model, while Section 3 describes the data. Section 4 performs an exploratory analysis of the data and the econometric results are presented in Section 5. Section 6 explores the implications, Section 7 offers a prospectus for future research, and Section 8 summarizes and concludes the paper.

2. Modeling Urban CO2 Concentrations

An extensive empirical literature has explored the determinants of CO2 emissions growth. Most of the attention has focused on drivers of CO2 emissions from fossil fuel combustion and cement production (e.g. Raupach et al., 2007; Jotzo et al., 2012). Land-use change also produces large CO2 emissions, which have been estimated more precisely by recent research (Gasser et al. 2020; Winkler et al. 2021). However, emissions drivers in this sector have received less attention than work on industrial determinants (Sanchez and Stern 2016). For both industrial and non-industrial sectors, previous studies have relied almost exclusively on estimates from CO2 emissions inventories that apply engineering parameters to measures of activity in industry, transport, land-clearing, residential heating and other sectors. Standard engineering estimates are particularly suspect for developing countries, because many of the parameters have been calibrated using databases and models developed for high-income economies.

This study takes a completely different approach, employing only direct CO2 observations from satellites. The dependent variable in our model is the atmospheric CO2 concentration above an urban area. For climate change analysis, the dominant concentration component is the global cumulative stock of long-duration CO2 molecules that have been emitted by human activity since the Industrial Revolution. Another global component is seasonal, reflecting differential CO2 absorption and respiration by vegetation over the annual cycle. The seasonal CO2 component is more pronounced in the Northern Hemispheric because it has more plant life than the Southern

Hemisphere. The third component is local, reflecting the time lag between local emissions of CO2 molecules and their full dispersion into the global mix. In this paper, we use the term "concentration anomaly" for the local component because it measures the deviation from the global background CO2 concentration.

Our model incorporates the two global components in a global time trend and controls for seasonality and hemisphere location. The local component comprises variables in three broad categories. The first includes activities in the most critical CO2-emitting sectors. The Intergovernmental Panel on Climate Change (IPCC) (Gale et al. 2005) has identified four dominant industrial sources of CO2 emissions: power plants, steel mills, cement plants, and oil refineries. Another potentially-important factor is atmospheric "spillover" from agricultural and forest burning in neighboring areas. Traffic emissions are also important, but we do not have reliable measures of motor vehicle operation for most of the cities in our sample.[1] The model therefore absorbs motor vehicle operations into the non-industrial income effects that are described below.

The second category includes demographic and economic variables. CO2 emissions should increase with urban population, ceteris paribus, because each resident accounts for some emissions. The spatial distribution of population may also play a significant role. In high-income areas that rely heavily on mechanized transport, increased population density may lower aggregate emissions by reducing travel requirements. On the other hand, higher population density in low-income areas may translate to higher CO2 emissions because small reductions in sparse mechanized transport do not offset increased CO2 emissions from factors like more concentrated household cooking and heating.

Economic development also has countervailing effects on CO2 emissions intensity. Higher-income urbanites use more goods and services, some of which are CO2-intensive (e.g., home heating, motor vehicles). However, locational economics inhibit CO2-intensive industrial activities in higher-income urban areas with higher land costs, fewer active resource mining sites, and stricter control of local air pollutants that are emitted along with CO2. In consequence, higher-income cities tend to import CO2-intensive goods and services from areas where the converse conditions hold. The net effect of urban economic development on CO2 emissions depends on the relative strength of direct income effects and indirect displacement and pollution control effects. Empirical research on the relationship between CO2 emissions and income has relied almost entirely on country-level emissions inventories. The results are mixed; some studies find a linear relationship, while others identify an inverse U-shaped relationship, or Environmental Kuznets Curve (EKC) (Ben Youssef, Hammoudeh and Omri 2016; Dasgupta et al. 2002). Where the EKC holds, domination passes from direct effects to displacement and pollution control effects as income rises. With satellite-based CO2 measures, the EKC investigation in this paper departs from conventional practice by avoiding emissions inventories and focusing on local rather than national CO2 emissions.

Climate comprises the third category. Other things equal, we would expect greater annual heating-related CO2 emissions from cities in cold climates.

We specify a linear estimation model because the atmospheric CO2 load should be additive in CO2 emissions from different sources. Spatially-referenced variables in the model are translated to

[1] Recent research has used Google Traffic to produce high-resolution traffic congestion data for individual cities (Dasgupta et al. 2021; Heger et al. 2018). Future research could extend this approach to all global cities.

consistent measures by resampling to centroids for grid cells with a resolution of 10 km. We allow for measurement "spillover" as emissions diffuse from source cells to neighboring grid cells.

We incorporate all of the previously-mentioned factors in our estimation model:

$$C_{it} = \beta_0 + \beta_1 t + \sum_{1}^{12} \gamma_m D_m + \sum_{1}^{12} \theta_m D_m L + \beta_2 P_{Ci} + \beta_3 P_{Gi} + \beta_4 P_{Oi} + \beta_5 S_i + \beta_6 R_i + \beta_7 B_i + \beta_8 F_{it} + \beta_9 N_{it} + \beta_{10} n_{it} + \beta_{11} n_{it}/\log(y_{it}) + \beta_{12} y_{it} + \beta_{13} y_{it}^2 + \beta_{14} H_{it} + \varepsilon_{it}$$

Expected signs: $\beta_1, \beta_2, \ldots \beta_9 > 0$, $\beta_{10} < 0$, $\beta_{11}, \beta_{12} > 0$, $\beta_{13} \leq 0$, $\beta_{14} > 0$.

For city i on date t:

C	=	Satellite-measured CO2 concentration
t	=	Elapsed days in the panel
D_m	=	Month dummy variable
L	=	Hemisphere dummy variable (0 = Southern; 1 = Northern)

Emissions from sectoral sources

P_C	=	Coal-fired power plants
P_G	=	Gas-fired power plants
P_O	=	Oil-fired power plants
S	=	Non-electric steel and iron plants
R	=	Oil refineries
B	=	Cement plants
F	=	Agricultural and forest fires

Demographic and income determinants

N	=	Population
n	=	Population density
y	=	Income per capita

Climate

H	=	Heating degree days

ε	=	Random error term

Our prior expectations for parameter signs are positive for elapsed time (β_1), sectoral activity ($\beta_2, \ldots \beta_8$) and population (β_9). Our population density specification has two terms, density (β_{10}) and density interacted with inverse log income (β_{11}). Sign-switching can occur for the case [$\beta_{10} < 0$, $\beta_{11} > 0$], where the first (negative) term dominates for high incomes and the second (positive) term

dominates for low incomes. We use inverse log income because the log transformation increases our ability to differentiate effects at very low income levels.

For the relationship between CO2 concentration and income per capita, we expect ($\beta_{12} > 0$). In the income-squared term, we expect $\beta_{13} < 0$ (the EKC case) or $\beta_{13} = 0$ (a linear relationship). Heating requirements are greater in colder climates, so we expect the effect of heating degree days on CO2 emissions (β_{14}) to be positive.

Clearly-exogenous variables in the model include fires in neighboring areas and the demographic and climate factors. We include georeferenced data on CO2-intensive industrial facilities because they should have important effects on observed CO2 concentrations above their locations. Their inclusion serves our principal objective, a relatively complete econometric accounting of city-level CO2 emissions that can be used for comparative performance benchmarking and exploration of residuals. However, we recognize the possibility of some estimation bias from interactions with income and local air pollutants. Industrial facilities emit locally-significant air pollutants (e.g., NO2, SO2, fine particulates) along with CO2. Technical measures to reduce local air pollutants (e.g., stack scrubbers for SO2 emissions) do not reduce CO2 emissions directly, but the associated costs may have significant indirect effects by altering facility location decisions. Stricter environmental regulation in higher-income cities may enhance this effect. In principle, we could treat the potential bias problem by using measures for input costs to instrument the facility-level variables. In practice, however, we have no prospect of measuring the relevant variables at the requisite spatial resolution. Joint determination of income and CO2 emissions could also be a significant problem for the EKC component of the model. Our results discussion will include some estimation exercises that shed further light on these issues.

3. Data

3.1 Sources

Several satellite platforms provide CO2 measures (Pan et al. 2021, Table 1). Data from these platforms have been collected by different instruments, over different periods, with different resolutions, observation repeat cycles and widths of area coverage along orbital paths. The data are also accessible in varying degrees. Combining observations from multiple sources could present difficulties that are as yet little-explored. For this exercise, prudence has dictated the choice of one platform, NASA's OCO (Orbiting Carbon Observatory)-2. We have chosen OCO-2 because it offers open access (JPL/NASA 2021); a long panel of consistently-measured daily observations (Sept. 6, 2014 – Dec. 31, 2020); and the highest spatial resolution among the available sources (1.29 × 2.25 km).

The design of OCO-2 supports comparative exercises like our analysis. It follows a sun-synchronous near-polar orbit, crossing the equator in ascending mode around 1330 hours local time. In practice, this means that the OCO-2 observations for our study are collected between 1200 and 1500 local time for all cities in the sample. This provides a consistent mid-day activity benchmark for comparing CO2 concentration anomalies across cities.[2] OCO-2 has an observation repeat time

[2] CO2 measurement during the full daily activity cycle will improve as systems like OCO-3 observe each area at more widely-varying times.

of 16 days We have downloaded georeferenced measures of XCO2 (the column-averaged dry air mole fraction of CO2) and computed daily mean values for each 10 km grid cell in our global database.

We use georeferenced facility-level global databases to obtain capacity measures and technology specifications for power plants (Byers et al. 2021), steel mills (GEM 2021), cement plants (McCaffrey et al. 2021), and oil refineries (Auch 2017). We use capacity estimates in the regressions because production estimates are both scanty and assigned low confidence by the database producers. Van der Werf et al. (2017) provide monthly estimates of carbon emissions from agricultural and forest burning at 25 km resolution.

The World Cities Database (2021) provides data on urban centroid locations and populations. Population density data are provided at 5 km resolution by CIESIN (2018). We use two sources to construct our georeferenced measure of income per capita. From the G-Econ database (Nordhaus et al. 2006), we obtain GDP per capita in 2005 purchasing power parity for a global grid with 100 km resolution. Each grid cell is assigned to its geographically-dominant country by G-Econ. For each cell in a country, we compute the ratio of cell GDP per capita to the national mean for all cells. We merge the results with annual World Bank estimates of GDP per capita in constant $US 2015, and use the cell ratios to estimate annual GDP per capita for each cell. We introduce another proxy for economic activity by incorporating monthly observations for VIIRS global nighttime lights (EOG 2021) at 500 m resolution. Mistry (2019) has provided global estimates of monthly heating degree days at 25 km resolution.

3.2 CO2 Diffusion Effects

Space-based observations detect higher CO2 concentrations over significant emissions sources because atmospheric diffusion is not instantaneous. As emissions diffuse from their sources, deviations from background concentrations will persist for some distance. By implication, the effects of emissions sources in the model should not be constrained by arbitrarily-scaled grid structures. To allow for diffusion, we incorporate the assumption that deviations from background CO2 concentrations are inversely related to distances from emissions points. We search for best-fit inverse-distance functions in regression experiments with distance exponent values from 0.1 to 3.0. We obtain the best results with an exponent that is effectively 1.0. It does not differ significantly across model variables, which simply confirms that CO2 molecules behave identically in the atmosphere, whatever their source. For estimation, the effect of an emissions source on satellite-measured CO2 concentration has unitary weight at its location and inverse-distance weights at the centroids of neighboring cells. For tractability, we bound the weighting radius at 100 km (where the weight is .01).

3.3 Wind Effects

Our modeling approach uses grid search experiments to determine distance decay functions for CO2 emissions from all geolocated sources (power plants, steel mills, cement plants, refineries, agricultural and forest burning). To illustrate the consequence, a capacity observation for coal-fired power plants at each 10-km grid centroid is the sum of inverse-distance-weighted capacities of coal-fired plants within a 100-km radius. At each point in time, the trajectory of emissions from each plant is potentially influenced by the wind direction at its location. However, we aggregate information from plants that may be widely separated, with a different wind direction at each plant.

In many urban areas (particularly in developing countries), the prevailing wind direction is regularly recorded at only one location (typically the airport). Taken together, the scarcity of wind direction information and aggregation of capacity measures across dispersed facilities in different micro-climates eliminate any chance of incorporating meaningful wind effects. Of course, all locations in some urban areas may be subject to identical wind-direction effects during some periods, in which case radially-symmetric inverse-distance weighting would generate errors for some observations. However, our study calculates daily averages from hourly data, with consequent summation over random changes in wind directions for multiple, widely-scattered points over five annual cycles. Some measurement error probably remains, but we believe that it compares favorably with measurement errors for other variables in our model (e.g., facility capacities, local heating degree days, neighboring fire locations).

3.4 Urban Scale

How many grid cells should be assigned to each city in our sample? Comparative analysis must confront the difference between arbitrary administrative boundaries and the actual extent of urban economic regions. Any attempt to define the latter will also include an arbitrary element. For all cities in this exercise, we standardize by including grid cells that lie within the same radial distance from their centroids. Then we test the robustness of the model by varying the radial distance. Another possible approach involves identification of a functional urban area (FUA) for each city region, as in Schiavina et al. (2019). FUAs are identified from urban mobility data for the OECD and Colombia, and estimated for other cities using a machine learning algorithm trained from estimated travel times, population distributions and incomes. We provide a further robustness test by estimating the model for FUAs as well.

4. CO2 Measures across Cities and over Time

4.1 Annual CO2 Concentrations

The global reference standard is provided by CO2 measurement at Mauna Loa Observatory, Hawaii (Keeling et al. 1976; Thoning et al. 1989). Table 1 compares mean annual December measures from Mauna Loa and our global OCO-2 database.[3] The results correspond closely, showing an increase from 399 ppm in 2014 to 414 in 2020.

Table 1: Annual global CO2 concentrations (ppm) (December)

Year	OCO-2	Mauna Loa
2014	399	399
2015	401	402

[3] Mauna Loa is in the Northern Hemisphere, so we compare its measures with Northern Hemisphere values from OCO-2.

2016	405	405
2017	406	407
2018	409	409
2019	411	412
2020	414	414

4.2 Hemispheric Seasonal Cycles

As previously noted, global CO2 concentrations fluctuate seasonally with CO2 absorption and respiration by vegetation over the annual cycle. Seasonal fluctuations are more pronounced in the Northern Hemispheric because it has more plant life. To measure the amplitude of CO2 cycles in the OCO-2 data, we regress measured CO2 on a time trend and compute monthly mean residuals for the Northern and Southern Hemispheres. Figure 1 displays mean residuals by month. The cycle is pronounced in the Northern Hemisphere, with the peak in April, the trough in August, and an annual amplitude of 7.5 ppm. The Southern Hemisphere cycle is much flatter, with the peak in July, the trough in March, and an annual amplitude of 1.5 ppm.

4.3 City Concentration Anomalies

In our model, differences in cities' economic, demographic and geographic conditions affect residual variations in measured CO2 once global trend growth and seasonal fluctuations are accounted for. We assess the scale of these concentration anomalies by computing residuals from a regression of CO2 on a time trend and hemispheric dummy variables for months. Figure 2 displays the distribution of mean anomalies for the cities in our sample, with a standard deviation of 1.0 ppm, 94.8% of cities in the range [-2,2] ppm and 98.5% in the range [-3,3] ppm. For comparison, human activity currently generates about 40 gigatons of CO2 emissions each year, increasing the atmospheric CO2 concentration by about 2 ppm. The city concentration anomalies in Figure 2 have the same order of magnitude, thus highlighting the global significance of inter-city variation.

Methods for direct conversion of city residuals to CO2 emissions are still in the research phase. Several recent studies (e.g. Ye et al. 2020; Wu et al. 2020) compare OCO-2-based city concentration anomalies ($\Delta CO2_{OCO2}$) with anomalies ($\Delta CO2_{E}$) estimated by combining atmospheric transport models with city-level data from global emissions inventories (principally ODIAC (Oda, Maksyutov and Andres 2018)). For the scaling factor [$R=\Delta CO2_{OCO2}/\Delta CO2_{E}$], Ye et al. (2020) find values of 1.6-1.9 for Riyadh, 2.4-2.9 for Cairo, and 2.9-3.2 for Los Angeles. In all three cases, city concentration anomalies calculated from standard emissions inventories significantly underestimate the anomalies in OCO-2 observations. These discrepancies may incorporate errors in sector-level activity data or emissions parameters employed by emissions inventories, as well as exclusion of some sectors from the inventories. For each city studied, a mid-range R-factor could be used to adjust its inventory-based emissions estimate.

Over time, accurate estimation of R-factors for more cities may permit larger-scale adjustment of urban CO2 emissions inventory estimates. The research reported in this paper contributes by quantifying the incremental contributions of multiple sectors to city-level OCO-2 concentration anomalies. Follow-on research could construct sector-level R-factors for adjusting emissions inventories at the sector level. Longer-term, R-factor research may succeed in dropping its current dependence on emissions inventories and produce methods for direct estimation of CO2 emissions

from satellite-measured CO2 concentration anomalies. At present, however, this domain remains largely unexplored.

Figure 1: Seasonal CO2 cycles in the Northern and Southern Hemispheres, Monthly deviations from trend (ppm)

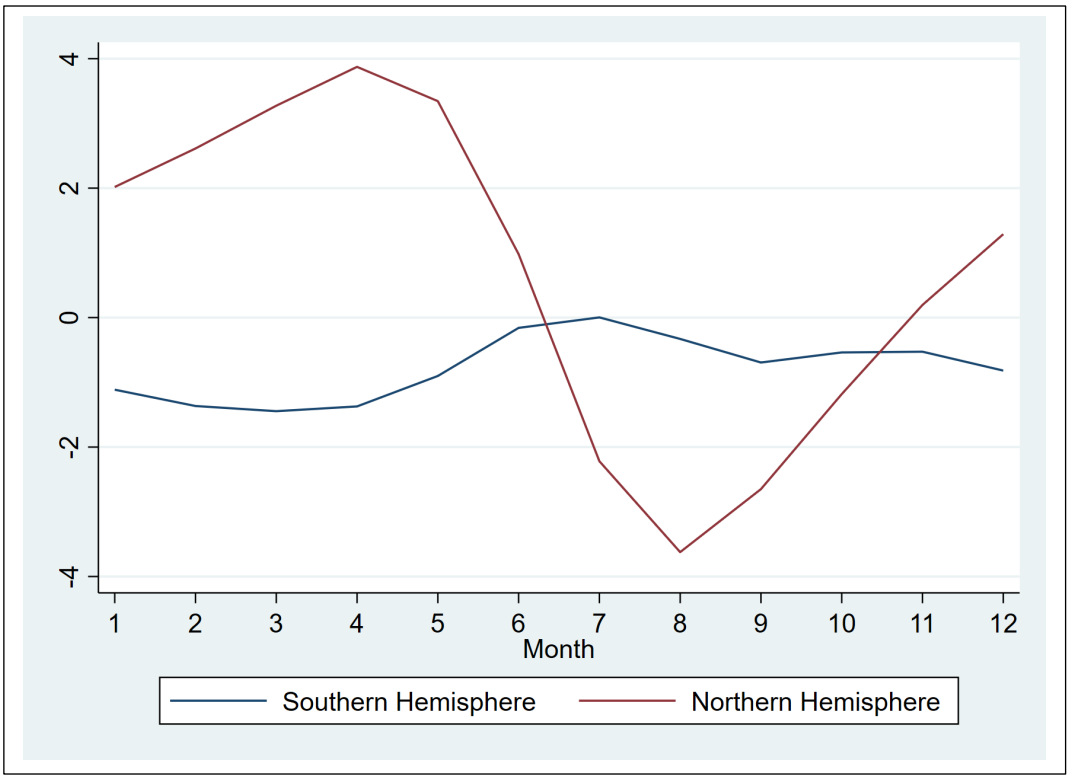

Figure 2: Distribution of mean residuals for cities

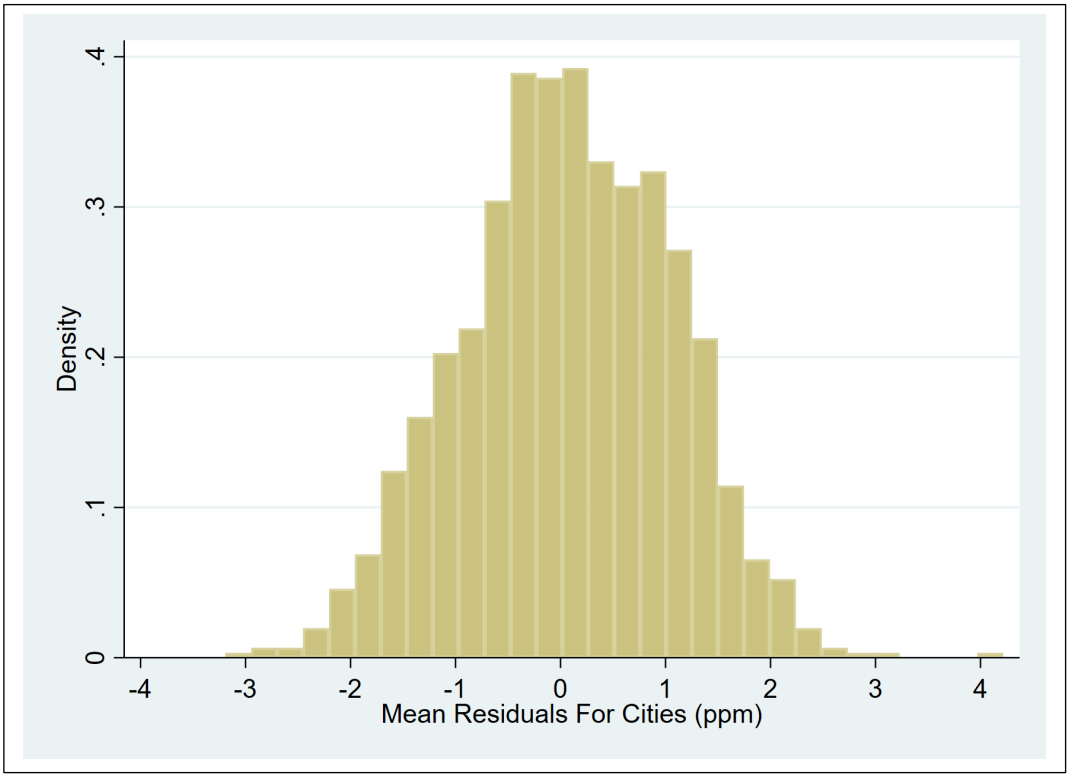

4.4 Sources of CO2 Emissions Variation across Cities

Before the formal econometric analysis, we explore descriptive evidence on three potential sources of variation in urban CO2 emissions.

Population

As previously noted, CO2 emissions should increase with urban population because each resident accounts for some emissions. We divide our sample cities into three size ranges with lower bounds at 500,000, 2,000,000 and 5,000,000 and compute mean CO2 concentration anomalies for the cities in each range. As Figure 3 indicates, mean anomalies increase with population size range. Population variation is associated with city anomaly variation over a range of 0.7 ppm, which is 0.7 standard deviation for the overall urban CO2 anomalies displayed in Figure 2.

Figure 3: Mean CO2 anomaly by city population size range

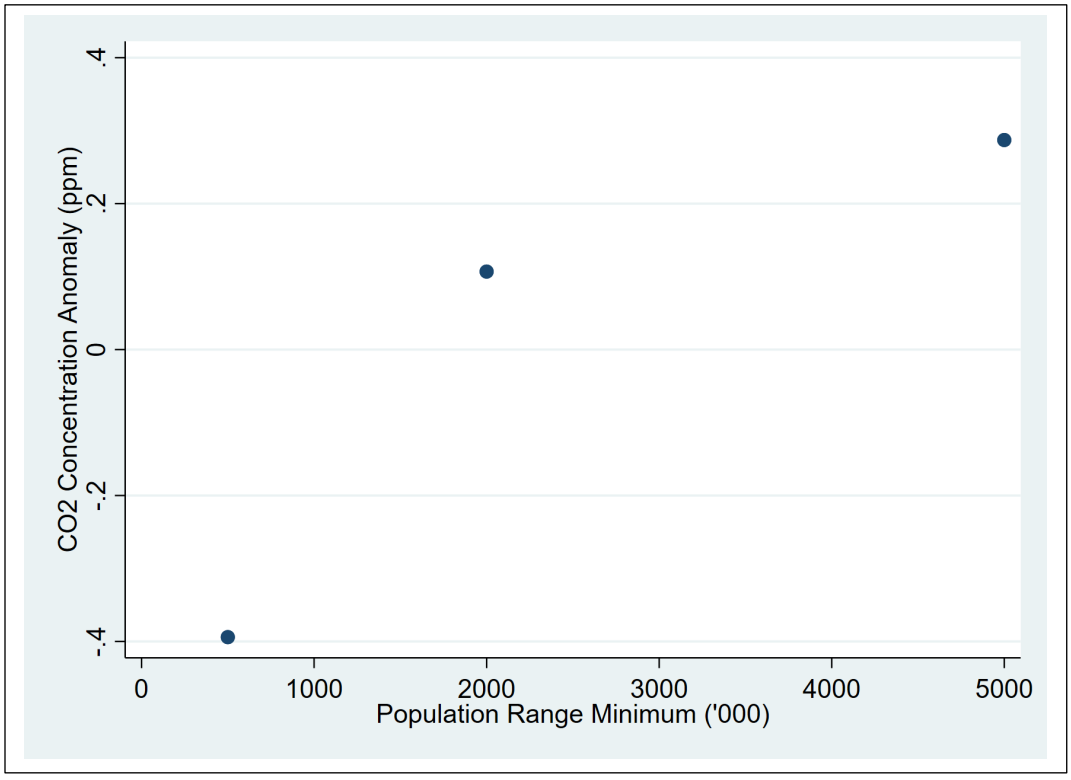

Industry Structure

For this exploration, we combine information on capacity in each city for industrial facilities in six categories: power plants fired by coal, gas and oil; non-electric steel mills; refineries; and cement plants. We normalize capacity in each category to the range [0 – 100][4] and compute total normalized capacity for the six sectors in each city. We compute mean CO2 anomalies for cities in five capacity

[4] For each sector, we identify the maximum capacity across sample cities. We divide capacity in each city by the sector maximum and multiply by 100.

ranges. Figure 4 shows a positive relationship between CO2 anomaly and aggregate capacity in CO2-intensive facilities, with capacity variation associated with anomaly variation over a range of 1.0 ppm, which is 1 standard deviation for the overall urban CO2 anomalies displayed in Figure 2.

Figure 4: Mean CO2 anomaly by CO2-intensive plant capacity

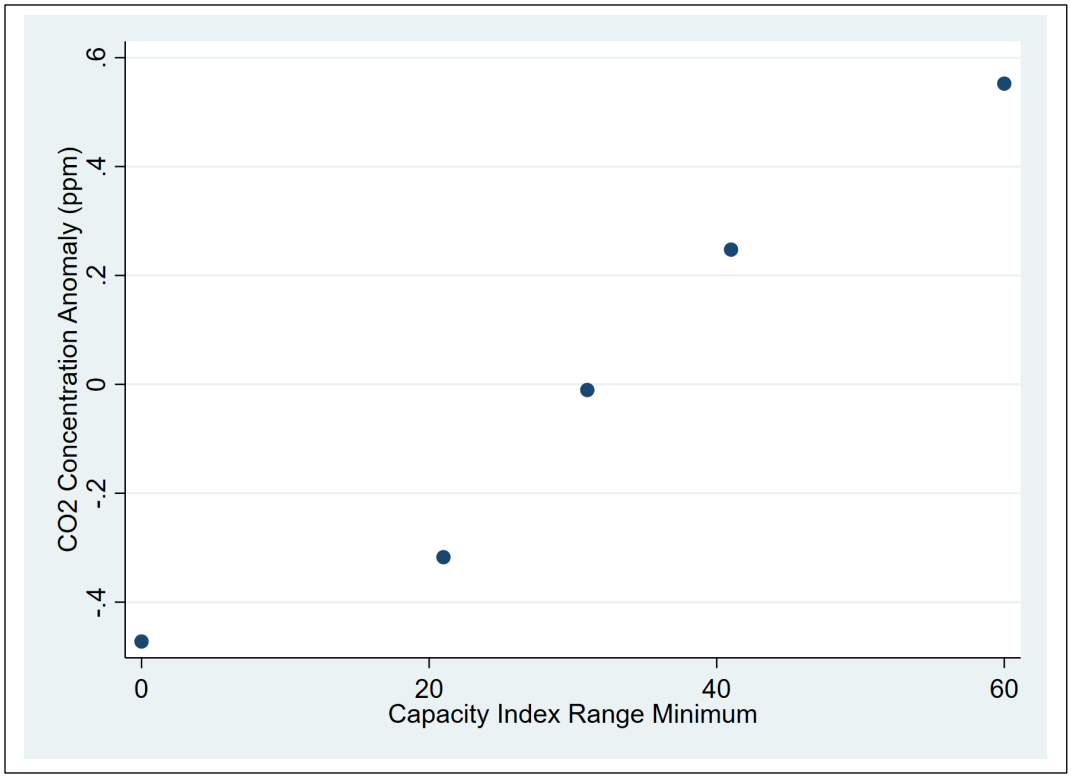

Economic Development

We divide cities into five ranges of income per capita ($US 2015) with upper bounds at $US [4,000 11,000 25,000 50,000 100,000]. Figure 5 shows that the association between mean CO2 anomaly and income per capita is consistent with an Environmental Kuznets Curve in which CO2 emissions increase to an upper bound in the range [$US 40,000-50,000] and then decrease. In Figure 5, sample variation in city per capita income is associated with variation of 1.6 ppm, or 1.6 standard deviation for the overall urban CO2 anomalies displayed in Figure 2.

Figure 5: Mean CO2 anomaly by city income per capita

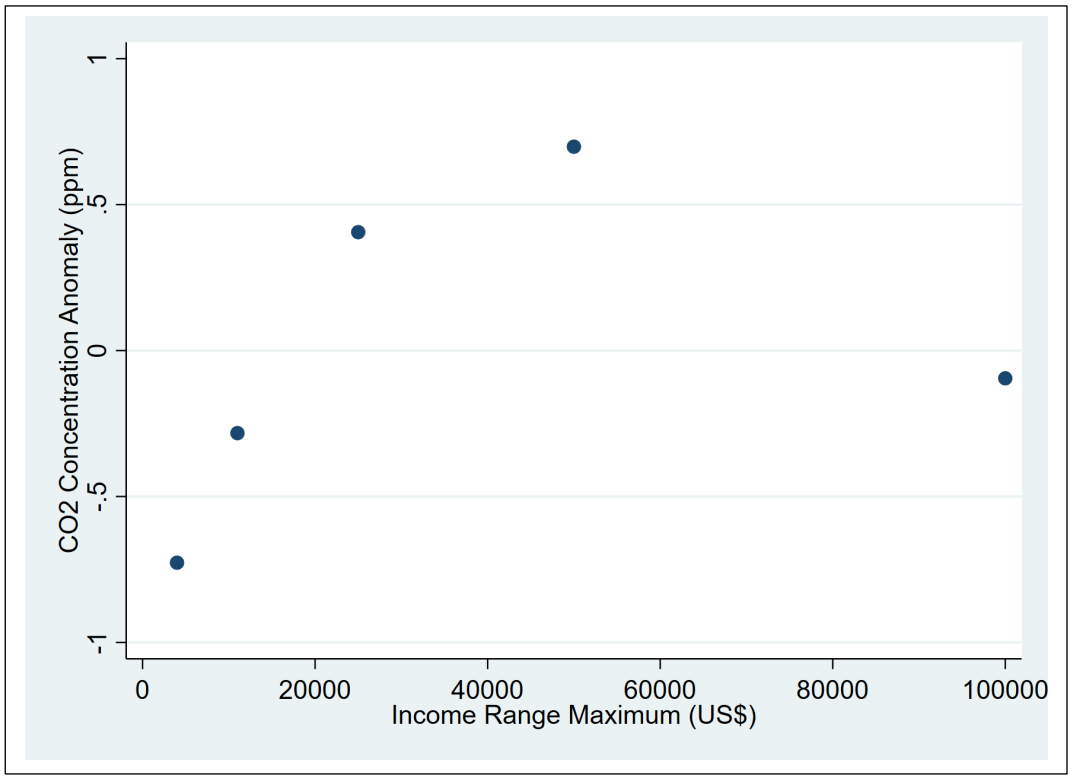

To summarize, our explorations suggest that sample variations in population, CO2-intensive industry scale and income per capita are associated with variations in mean urban CO2 anomalies of 0.8, 1.0 and 1.6 standard deviations. Taken together, these associations suggest that the three factors account for a significant component of variation among the sample cities. Strong inferences cannot be drawn because the three factors are not statistically independent (sample correlations: [population/plant capacity 0.22]; [population/income 0.02]; [income/plant capacity 0.51]. In addition, our aggregative measure of plant capacity imposes an implicit assumption of equal sectoral impact that may not be warranted. For more systematic evidence, we turn to the results of our econometric estimation.

5. Model Estimation Results

Table 2 reports our regression results for radial distances of 20, 40 and 60 kilometers, as well as cells within 60-km radii that also lie within Functional Urban Areas. We present results for OLS and HAC[5] panel estimation, which adjusts standard errors for spatial autocorrelation. We have scaled the variables to yield easily-reportable parameter estimates (i.e., estimates with limited leading zeros after the decimal place); units are included for each variable.

Overall, we find that the model provides a good fit to the data. The results are highly robust to variations in radial distance and cell restriction to Functional Urban Areas, with the expected signs

[5] Heteroscedasticity and autocorrelation consistent.

and generally-high levels of statistical significance for all model variables. At the same time, the cities in our sample display broad variation in regression residuals after the model variables are taken into account. This suggests a potentially-important domain for climate-related policies, and Section 6 explores one policy dimension with an analysis of the relationship between urban mass transit investments and the regression residuals.

Our comparative results for power facilities are consistent with prior expectations: Coal-fired power has the greatest impact on atmospheric CO2 concentration, followed successively by oil-and gas-fired power. Non-electric steel/iron complexes, cement plants and refineries have generally-high significance, along with agricultural and forest burning in neighboring areas. We have incorporated the VIIRS nighttime light illumination index as an additional proxy for economic development; all results have similar parameter estimates, the expected signs, and high significance. Heating degree days also has the expected sign and high significance in all cases.

5.1 Population Effects

Population has the expected positive, highly-significant effect on CO2 concentration. The results for population density and its interaction with inverse log population are consistent with sign-switching as income rises. Figure 6 displays the estimated relationship between income per capita and the composite density parameter $[\beta_{10} + \beta_{11}/\log(y)]$. It suggests that sign-switching occurs around $US 1000, where the composite density parameter is equal to 0.

Figure 6: Regression population density parameter vs. income per capita

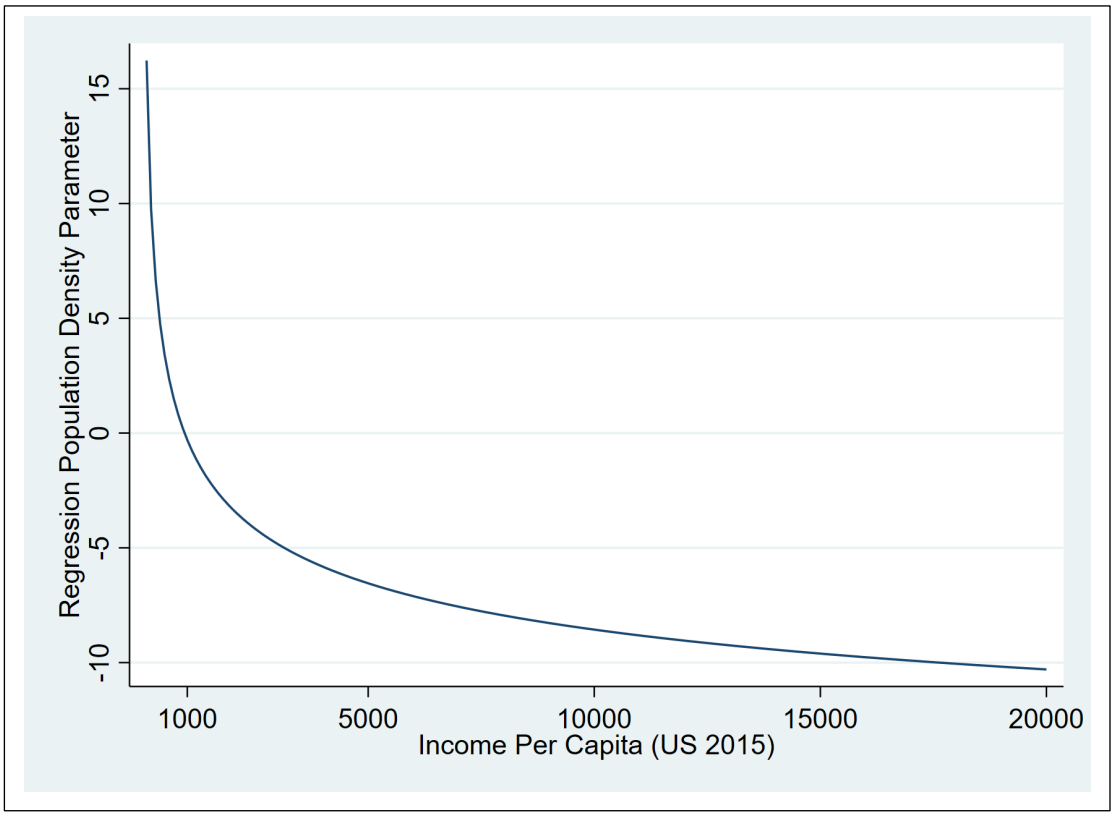

Figure 7 illustrates the implications by displaying the density/CO2 relationship as income increases. The relationship is strongly positive at $US 400 per capita and mildly so at $US 800. Then it switches sign and becomes progressively more negative for $US 1200, 2000 and 5000.

These population density results may be of interest for the discussion of optimal timing in urban development strategy. In our interpretation, they do not imply that low-income cities should not exploit opportunities for higher-density development, because pursuing such opportunities may help them avoid locking into carbon-intensive residential and infrastructure patterns that are difficult to reverse as income increases. However, our results do imply that CO2 increases may accompany the first phase of densification for some low-income cities.

Figure 7: CO2 anomaly (ppm) vs population density at different income levels

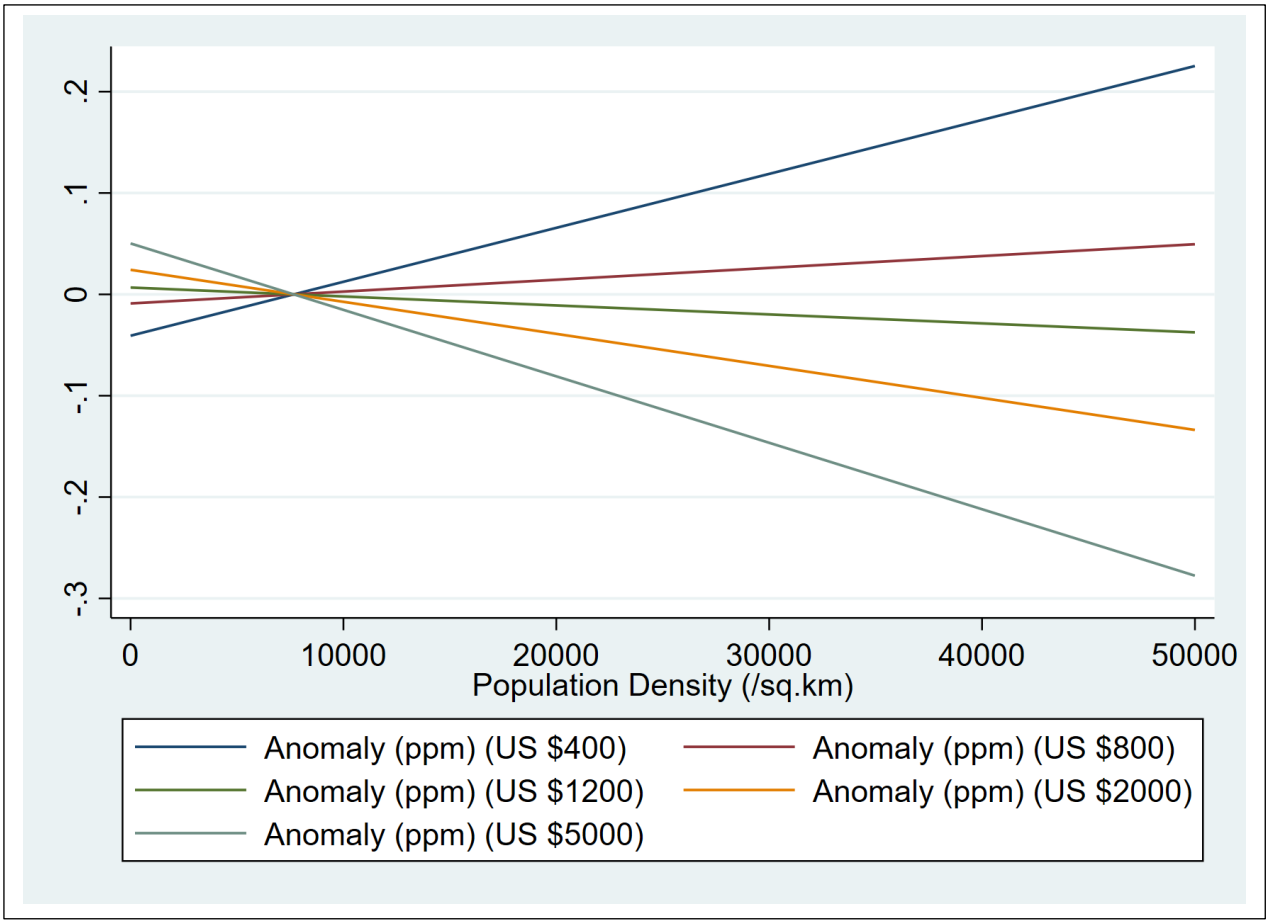

5.2 Income Effects

Our results for income per capita are highly significant and consistent with an Environmental Kuznets Curve (EKC) for urban CO2 emissions ($\beta_{12} > 0$, $\beta_{13} < 0$). In supplementary exercises, we have addressed issues related to (1) potential biases associated with inclusion of emissions-intensive facilities; (2) inclusion of an income-interactive term in the population density component; and (3) simultaneity in the relationship between CO2 emissions and non-industrial income factors. For case

(1), we have estimated regressions that exclude either industrial emissions sources or income. When we exclude the income terms, we find a very small effect (median change of 3%) on parameter estimates for power plants, steel mills, cement plants and refineries. When we exclude the industrial facilities, we find that the income parameters change slightly. For case (2), we have estimated regressions that exclude all righthand variables except income, time trend and seasonal controls (by hemisphere). As expected, with all collinear variables dropped, we find an increase in the significance and size of the EKC parameters.

Figure 8 displays the estimated EKC with industrial emissions sources, without them (case 1), and without any righthand variables except the EKC terms (and the trend and seasonal controls) (case 2). With industrial sources excluded, the EKC peaks sooner and declines more sharply at higher incomes. At present, we cannot say how much of this change reflects estimation bias and how much reflects the collinearity-related upward bias that would accompany exclusion of properly-instrumented facility variables. In any case, all three estimates carry the same basic message: The EKC reaches a peak in the range [$40,000 - $50,000] which is above the 90th percentile internationally.

Case (3) warrants more detailed attention because of potential simultaneity bias in the relationship between income and CO2 emissions. A substantial literature has used inventory-based emissions estimates to study this relationship at the country level (e.g., Apergis and Payne 2014). Results have differed substantially by country and time period (Ben Youssef et al. 2016). The research presented in this paper is different from previous work in at least three relevant ways. First, it uses direct, satellite-based observations of CO2 rather than estimated emissions inventories. Previous studies have risked introducing some technical element of simultaneity *by construction*, because their emissions inventories derive entirely from measures of activities that provide components of income. Second, the present study uses local, spatially-referenced data rather than national or regional aggregates. Third, we take a different approach to energy as a link between income and CO2 emissions. Most previous studies of the simultaneity issue have focused on the energy sector as the key determinant of simultaneity between income and CO2 emissions, because CO2 emissions increase with energy use and energy use contributes to economic growth. Researchers' views have differed substantially on the potential importance of this problem. Csereklyei and Stern (2015) argue that the bias is fairly small, so estimated emissions-income elasticities will be close to effects for exogenous changes in income. In any case, the modeling exercise in this paper takes an entirely different approach to the energy sector, incorporating georeferenced data for the coal-, gas- and oil-fired power plants that create sectoral CO2 emissions while excluding other power facilities (e.g., nuclear, solar, wind, hydro) that do not. In the previous subsection, we have discussed and illustrated the implications of our approach to energy facilities.

As previously noted, the EKC component of our model relates to non-industrial, income-related activities (e.g., motor transport) that cannot be observed directly. The relationship between income and CO2 emissions from these activities may also include elements of simultaneity, such as the joint emission by some activities of CO2 and local air pollutants (NO2, SO2, CO) that affect health, productivity, and therefore income (Van Ewijk and Van Wijnbergen 1995).

For econometric estimation, instrumental variables (IV) provide the standard correction for such simultaneity problems. In recent work on EKC estimation for local pollutants, Lawell and Liscow (2013) have identified the age dependency ratio as a plausibly-exogenous instrument that affects

economic growth via the savings rate and overall labor productivity. We have adopted this approach for a first-stage regression that relates national income growth since 2010 to the age-dependency ratio. We substitute the regression prediction for income per capita in our EKC model that excludes all other righthand variables except the time trend and seasonal variations by hemisphere. The resulting EKC estimate is included in Figure 8 (labeled "IV"). Its peak occurs at a lower CO2 anomaly than its OLS counterpart, and at an income that is substantially higher. We should emphasize that this IV result is far from the last word, and future research should use satellite-measured CO2 data to address the simultaneity issue in more depth.

We should also note that the income-related results in this study are only intended to provide a benchmark for judging urban performance in reducing CO2 emissions. The same would be true if our results had rejected the EKC ($\beta_{12} > 0$, $\beta_{13} = 0$), yielding a relationship in which CO2 emissions increase continuously with income per capita. To avoid any misunderstanding, we should emphasize that *our EKC results have no normative or policy implications in themselves*. They do not imply that additional public resources are not needed for reducing CO2 emissions because "the problem will take care of itself" with continued economic growth. In fact, the opposite is true. The most recent IPCC report (IPCC (2021), Figure SPM.10) affirms a near-linear relationship between cumulative CO2 emissions and the increase in global surface temperature. Our EKC results (Figure 8) show that even high-income countries have not approached zero CO2 emissions, and growing industrial giants like India and China are still on the rising portion of the curve. The clear implication is that waiting for the EKC to reduce emissions from all countries would produce an enormous increase in cumulative CO2 and a potentially-catastrophic global temperature increase. This conclusion will simply be compounded if future research finds insignificance for the EKC regression parameter ($\beta_{13} = 0$).

Finally, we should note that our EKC results only provide a descriptive "snapshot" of the income/emissions relationship for our sample urban areas during the period 2014-2019. Even if the EKC specification survives future econometric tests, policy changes and technology improvements may lower the EKC peak significantly while shifting it to a much lower income level. Indeed, it is possible that recent changes in policy and technology in wealthier economies have already steepened the post-peak decline in CO2 emissions at higher incomes. Tracking changes in the emissions/income relationship and its determinants should be an important topic for future research.

Figure 8: Alternative EKC estimates

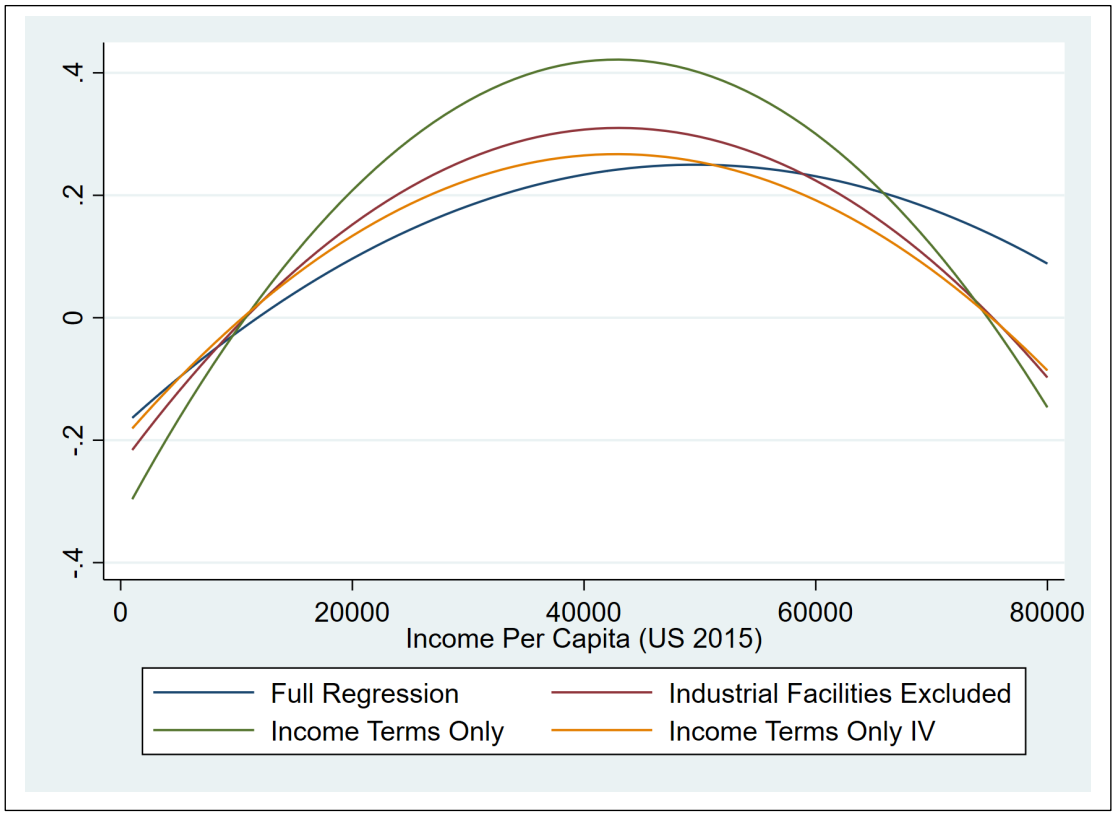

Table 2: Determinants of measured CO2 concentration (OCO-2 satellite platform): Cities with populations greater than 500,000

Urban Radius (km)	20		40		60		60 (FUA Only)	
Estimation	OLS	Spatial HAC	OLS	Spatial HAC	OLS	Spatial HAC	OLS	Spatial HAC
Power Capacity (Coal)	137.2***	134.1***	142.0***	137.7***	138.6***	133.2***	126.0***	118.1***
[Megawatts (`00,000)]	(28.75)	(20.74)	(45.24)	(32.28)	(51.49)	(35.88)	(35.50)	(25.48)
Power Capacity (Gas)	54.27***	48.02***	51.48***	41.96***	56.56***	48.56***	58.14***	53.58***
[Megawatts (`00,000)]	(8.58)	(5.55)	(11.74)	(7.00)	(15.71)	(9.84)	(13.81)	(9.66)
Power Capacity (Oil)	67.20***	110.9***	94.31***	128.2***	99.39***	125.6***	54.67***	82.82***
[Megawatts (`00,000)]	(4.45)	(4.86)	(9.70)	(9.52)	(12.08)	(11.05)	(6.06)	(6.86)
Non-Electric Steel and Iron Capacity	10.52***	9.900***	14.65***	13.86***	17.19***	16.33***	13.72***	13.24***
[Tonnes (‘00,000)]	(10.92)	(7.95)	(21.87)	(15.12)	(28.10)	(19.47)	(18.35)	(13.38)
Refinery Capacity	0.0857	0.0337	0.144**	0.105	0.218***	0.187***	28077.2***	26375.6***
[Barrels Per Day (’00,000)]	(1.19)	(0.36)	(3.23)	(1.69)	(5.81)	(3.52)	(6.97)	(4.72)
Cement Capacity	0.323***	0.332***	0.373***	0.400***	0.443***	0.476***	0.376***	0.384***
[Tonnes (‘000,000)]	(15.97)	(12.36)	(27.67)	(21.91)	(37.45)	(29.25)	(23.92)	(18.73)
Carbon Emissions, Ag and Forest Burning	1258.0***	1444.1***	435.9***	286.3***	499.9***	353.9***	167.3**	63.51
[[Grams Carbon/m2]/Month (’00,000)]	(4.63)	(5.36)	(6.27)	(4.19)	(10.44)	(7.49)	(2.64)	(1.04)
Population	0.0103***	0.0133**	0.0169***	0.0189***	0.0194***	0.0234***	0.0141***	0.0156***
[‘000,000]	(3.42)	(3.15)	(10.89)	(8.84)	(19.21)	(16.36)	(11.54)	(9.33)
Population Density [$US 0 – 300]	-32.42**	-47.45**	-33.35**	-49.77***	-32.68***	-53.35***	-10.09	-22.19
[‘000,000/sq. km]	(-2.72)	(-2.86)	(-3.19)	(-3.40)	(-3.32)	(-3.81)	(-0.99)	(-1.58)
Population Density / Log (Income Per Capita)	245.6**	328.7*	228.3**	351.0**	248.9**	425.6***	76.26	158.4
	(2.68)	(2.56)	(2.83)	(3.08)	(3.24)	(3.87)	(0.96)	(1.44)
Income Per Capita	0.216***	0.174***	0.175***	0.145***	0.143***	0.121***	0.146***	0.111***
[Constant 2015 $US ‘000]	(14.42)	(8.73)	(22.21)	(13.76)	(25.59)	(15.91)	(17.69)	(10.34)
$[\text{Income Per Capita}]^2$	-0.0228***	-0.0209***	-0.0176***	-0.0166***	-0.0136***	-0.0124***	-0.0156***	-0.0137***
	(-10.54)	(-7.34)	(-15.07)	(-10.76)	(-16.19)	(-11.06)	(-13.63)	(-9.26)

VIIRS Night Illumination Index	0.00263***	0.00397***	0.00426***	0.00518***	0.00457***	0.00447***	0.00435***	0.00403***
[Nanowatts/steradian]/cm2	(4.63)	(5.30)	(9.64)	(8.82)	(13.41)	(10.97)	(11.56)	(9.20)
Heating degree days	190.1***	272.7***	179.1***	258.2***	174.2***	253.2***	202.5***	278.1***
['00,000]	(31.94)	(40.74)	(59.07)	(74.99)	(81.30)	(103.52)	(49.81)	(61.48)
Observation Date	0.00705***	0.00705***	0.00703***	0.00702***	0.00701***	0.00700***	0.00700***	0.00700***
	(463.19)	(488.78)	(869.58)	(919.02)	(1217.74)	(1288.54)	(725.05)	(761.01)
February	-0.00877	-0.00946	-0.124	-0.112	-0.0347	-0.0636	-0.266*	-0.229*
	(-0.05)	(-0.05)	(-1.26)	(-1.22)	(-0.52)	(-1.01)	(-2.55)	(-2.34)
March	-0.115	-0.168	-0.119	-0.130	-0.0188	-0.0275	-0.0991	-0.102
	(-0.63)	(-0.99)	(-1.23)	(-1.46)	(-0.28)	(-0.45)	(-0.94)	(-1.03)
April	0.154	-0.0697	0.0878	-0.0749	0.100	-0.0171	-0.00432	-0.112
	(0.90)	(-0.43)	(0.97)	(-0.87)	(1.62)	(-0.29)	(-0.04)	(-1.17)
May	0.546**	0.301	0.461***	0.221**	0.555***	0.308***	0.194	0.0215
	(3.15)	(1.84)	(5.28)	(2.68)	(9.35)	(5.52)	(1.95)	(0.23)
June	1.225***	0.972***	1.141***	0.842***	1.154***	0.865***	0.747***	0.559***
	(7.31)	(6.13)	(13.57)	(10.53)	(20.23)	(15.99)	(7.60)	(5.98)
July	1.098***	0.888***	1.075***	0.835***	1.209***	0.963***	0.735***	0.550***
	(6.63)	(5.64)	(13.08)	(10.70)	(21.71)	(18.24)	(7.83)	(6.12)
August	0.862***	0.679***	0.796***	0.577***	0.856***	0.642***	0.564***	0.397***
	(5.11)	(4.24)	(9.44)	(7.22)	(14.95)	(11.86)	(5.89)	(4.35)
September	0.791***	0.600***	0.625***	0.478***	0.634***	0.504***	0.504***	0.388***
	(5.04)	(3.99)	(7.62)	(6.10)	(11.18)	(9.35)	(5.51)	(4.41)
October	1.194***	0.915***	0.894***	0.657***	0.899***	0.699***	0.688***	0.535***
	(7.42)	(5.89)	(10.53)	(8.08)	(15.31)	(12.47)	(7.22)	(5.80)
November	0.948***	0.714***	0.736***	0.546***	0.747***	0.618***	0.508***	0.408***
	(5.86)	(4.54)	(8.49)	(6.50)	(12.31)	(10.57)	(5.19)	(4.28)
December	0.419*	0.307*	0.175*	0.108	0.204***	0.173**	0.0823	0.0820
	(2.55)	(1.96)	(1.98)	(1.27)	(3.30)	(2.95)	(0.84)	(0.88)

January x [Northern Hemisphere]	3.408***	2.853***	3.124***	2.628***	3.039***	2.599***	3.040***	2.647***
	(24.37)	(20.76)	(43.28)	(37.06)	(61.01)	(53.14)	(38.12)	(33.57)
February x [Northern Hemisphere]	4.142***	3.643***	3.979***	3.514***	3.780***	3.419***	4.076***	3.717***
	(31.51)	(27.13)	(55.37)	(48.71)	(77.40)	(69.91)	(54.78)	(49.31)
March x [Northern Hemisphere]	4.896***	4.549***	4.658***	4.312***	4.483***	4.180***	4.533***	4.266***
	(38.10)	(35.92)	(67.55)	(63.49)	(93.78)	(88.77)	(59.31)	(56.25)
April x [Northern Hemisphere]	5.108***	5.027***	5.043***	4.938***	4.996***	4.878***	5.045***	4.962***
	(45.33)	(44.50)	(81.92)	(80.37)	(120.60)	(117.67)	(73.04)	(71.50)
May x [Northern Hemisphere]	4.407***	4.368***	4.241***	4.250***	4.088***	4.149***	4.367***	4.376***
	(38.67)	(38.26)	(75.88)	(75.36)	(109.52)	(109.59)	(65.27)	(65.09)
June x [Northern Hemisphere]	1.709***	1.680***	1.547***	1.610***	1.475***	1.571***	1.956***	1.982***
	(16.23)	(15.66)	(30.44)	(30.64)	(43.85)	(44.88)	(29.64)	(29.71)
July x [Northern Hemisphere]	-0.591***	-0.616***	-0.866***	-0.842***	-1.016***	-0.956***	-0.548***	-0.506***
	(-5.84)	(-5.93)	(-18.41)	(-17.18)	(-32.81)	(-29.32)	(-9.35)	(-8.38)
August x [Northern Hemisphere]	-2.337***	-2.370***	-2.434***	-2.398***	-2.424***	-2.357***	-2.313***	-2.251***
	(-21.76)	(-21.84)	(-47.44)	(-45.88)	(-70.77)	(-67.31)	(-37.12)	(-35.71)
September x [Northern Hemisphere]	-1.811***	-1.844***	-1.830***	-1.873***	-1.860***	-1.874***	-1.806***	-1.798***
	(-21.12)	(-20.96)	(-39.44)	(-39.57)	(-57.51)	(-56.81)	(-33.35)	(-32.65)
October x [Northern Hemisphere]	-0.567***	-0.695***	-0.525***	-0.646***	-0.622***	-0.733***	-0.415***	-0.531***
	(-6.16)	(-7.39)	(-10.31)	(-12.57)	(-17.50)	(-20.46)	(-6.91)	(-8.70)
November x [Northern Hemisphere]	0.917***	0.662***	0.919***	0.666***	0.822***	0.556***	1.164***	0.925***
	(9.73)	(6.76)	(17.00)	(11.95)	(21.14)	(13.98)	(18.08)	(13.97)
December x [Northern Hemisphere]	2.442***	1.918***	2.432***	1.946***	2.319***	1.858***	2.529***	2.092***
	(24.75)	(19.10)	(42.34)	(33.63)	(56.87)	(45.38)	(39.49)	(32.35)
Constant	254.3***	254.7***	255.0***	255.3***	255.4***	255.7***	255.5***	255.7***
	(736.01)	(775.48)	(1395.77)	(1472.50)	(1971.11)	(2080.00)	(1181.10)	(1235.86)
Observations	37,788	37,788	129,851	129,851	247,592	247,592	89,157	89,157

Absolute value of t statistics in parentheses
* significant at 5%; ** significant at 1% *** significant at 0.1%

5.3 Influence of Regression Variables on CO2 Emissions

We use standardized (beta) coefficients[6] to provide measures of relative importance for model variables. Table 3 presents results from our 40-km radial estimates, standardized to weights that add to 100. Overall, we find influence weights of 34.3 for industrial sources, 34.5 for measures of economic development, 10.6 for population-related factors, and 20.8 for environmental variables.[7] Among industrial sources, the top three by influence are coal-fired power (13.2), cement (7.3) and steel (6.2). For economic development, population factors and environmental variables, the top variables are income per capita, population density and heating degree days, respectively.

Table 3: Influence of variables on CO2 emissions

Industry	Influence (%)
Coal Power	13.2
Cement	7.3
Steel	6.2
Gas Power	3.9
Oil Power	2.8
Refineries	0.9
Subtotal	34.3
Economic Development	
Income Per Capita	31.5
Nighttime Lights	3.0
Subtotal	34.5
Population Factors	
Population Density	7.1
Population	3.5
Subtotal	10.6
Environment Factors	
Heating	19.0
Fires	1.8
Subtotal	20.8

[6] A beta coefficient transforms a regression coefficient to measure the change in the dependent variable, measured in standard deviations, for a standard deviation increase in the independent variable.

[7] The four subtotals have a total of 100.2 because of rounding to the first decimal point.

6. Discussion

6.1 Global Comparisons

Our regression model incorporates a host of determinants, including the annual global trend, seasonal changes by hemisphere, industry structure, fires in neighboring areas, demography, the income component that is uncorrelated with industry structure, and climate.

Regression Predictions and Residuals

Figure 9 maps regression-predicted mean CO2 anomalies for the 1,236 cities in the sample. The predictions vary widely in all major regions. China is distinguished, both by the number of cities and the high proportion of CO2-intensive cities in its eastern coastal region. Overall, however, Chinese cities display the same broad variation as cities in other regions.

The fitted model can provide a pilot template for judging cities' emissions performance. However, we should emphasize some particular features of model structure. First, it includes heavily-emitting industrial facilities but does not include clean power sources and electric arc steel production. Urban areas where industry has switched to these less-CO-intensive technologies will have lower actual and predicted emissions than cities with CO2-intensive technologies. In a related vein, although some urban areas may not have pollution-intensive power plants within the radial distances used for this study, they may import power from more distant pollution-intensive facilities. From a consumption perspective, such areas are not "cleaner" than areas with local power production. We provide these cautionary notes because our model is explicitly intended to "level the playing field" by treating facilities like pollution-intensive power plants as historical legacies that provide benchmarks for judging future performance. Our model estimates for industrial facilities establish fixed initial conditions, while automatically adjusting for the continuing global trend, seasonal fluctuations, changes in nearby fires, temperature changes, and changes in population and income.

Some insight into cities' current status can be gained by examining their mean regression residuals, which provide a measure of their deviations from regression predictions during the sample period. Figure 10 maps regression residuals for the 1,236 cities in the sample, while Figure 11 displays boxplots of residual distributions by region.[8] The map displays wide variation in all regions, but certain regional patterns suggest deviations from collective global experience. The number of large positive residuals in China is apparent, while large negative residuals are strongly evident in the former Comecon countries.[9] Figure 11 confirms the impression for China. Despite a wide dispersion of positive and negative residuals, China's median is about .5 ppm (or .5 standard deviation for cities' local component) above the global norm (a residual of 0). Distributions lying above the global norm are also evident for the other countries in East Asia & Pacific, Sub-Saharan Africa, and Middle East & North Africa. North America, Latin America & Caribbean, and South Asia (excluding India) have wide distributions that are roughly centered around 0. The medians for

[8] The upper and lower box boundaries are quartile values; interior lines are medians. A few extreme values in each region have been excluded for ease of interpretation.

[9] The countries of the former Soviet Union and associated countries in Eastern Europe.

India and Western Europe are about 0.5 standard deviation below the global norm, while the median for the former Comecon countries is more than 1 standard deviation below the norm.

More detailed information about city distributions by region is provided in Appendix tables A1-A10, which tabulate the cities in each region that have 15 negative and 15 positive residuals with the largest absolute values. These are the cities whose measured CO2 emissions are notably smaller or larger than expectation, as measured by the regression predictions. For each city, the tables present measured CO2 for the sample period, model-predicted CO2, and the residual.

Source Decomposition of Predicted CO2

The Appendix tables also use the regression results to decompose predicted CO2 emissions into five source categories: Industry (power plants, steel mills, refineries, cement plants); Fires (carbon emissions from agricultural and forest burning); Income (non-industrial CO2 sources that are correlated with income); Population (population and population density); and Climate (heating degree days). Figure 12 maps illustrative decompositions for the sample cities. Particularly important roles are suggested for Fires in Sub-Saharan Africa and Climate in northern Asia, the Russian Federation and Eastern Europe.

Table 4 tabulates mean shares by region for each source sector. Cities in India, China and other East Asia & Pacific countries have mean Industry shares above 40%; Sub-Saharan Africa has the largest share for Fires; Latin America & Caribbean, North America and Western Europe have dominant shares for Income (the income component that is uncorrelated with Industry); Sub-Saharan Africa, India and other South Asian countries have dominant shares for Population, while the former Comecon countries have by far the largest mean share for Climate.

Figure 9: Regression-Predicted CO2 concentration anomalies (ppm)
Global cities with populations > 500,000

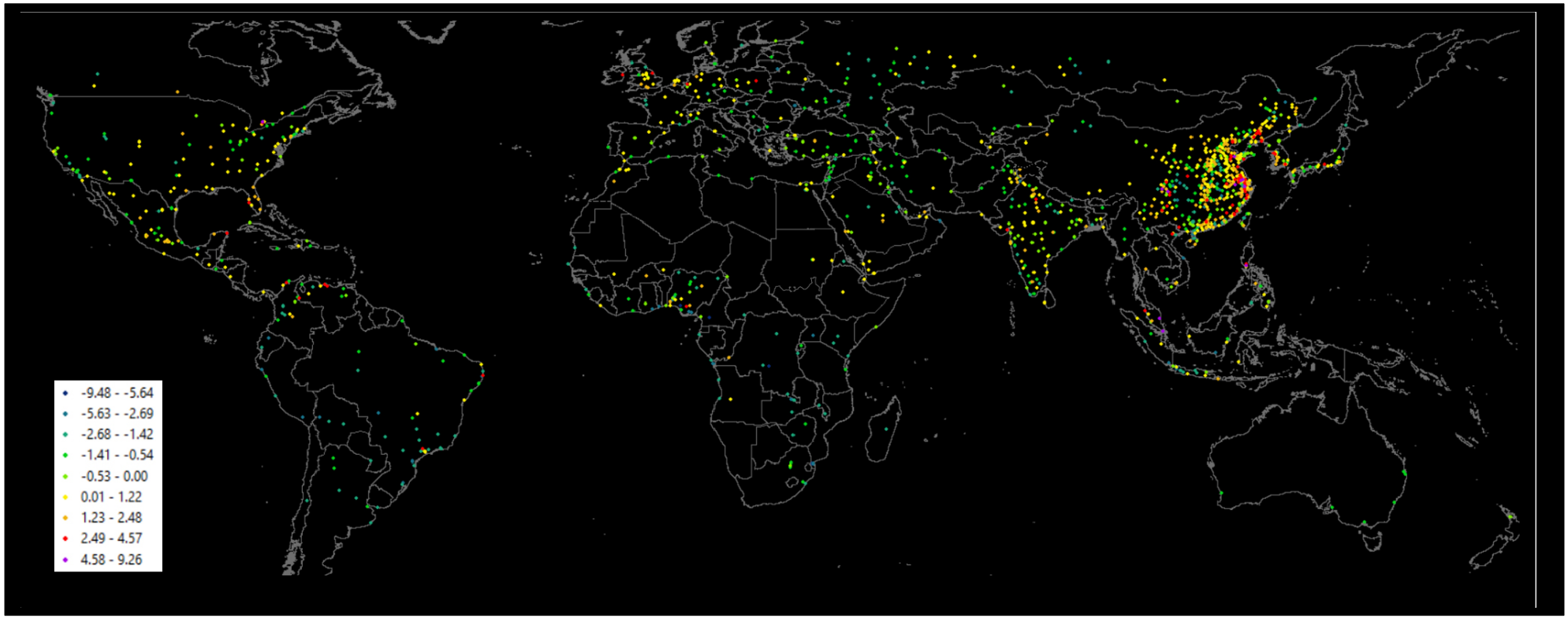

Figure 10: Residuals from Regression-Predicted CO2 concentrations (ppm)
Global cities with populations > 500,000

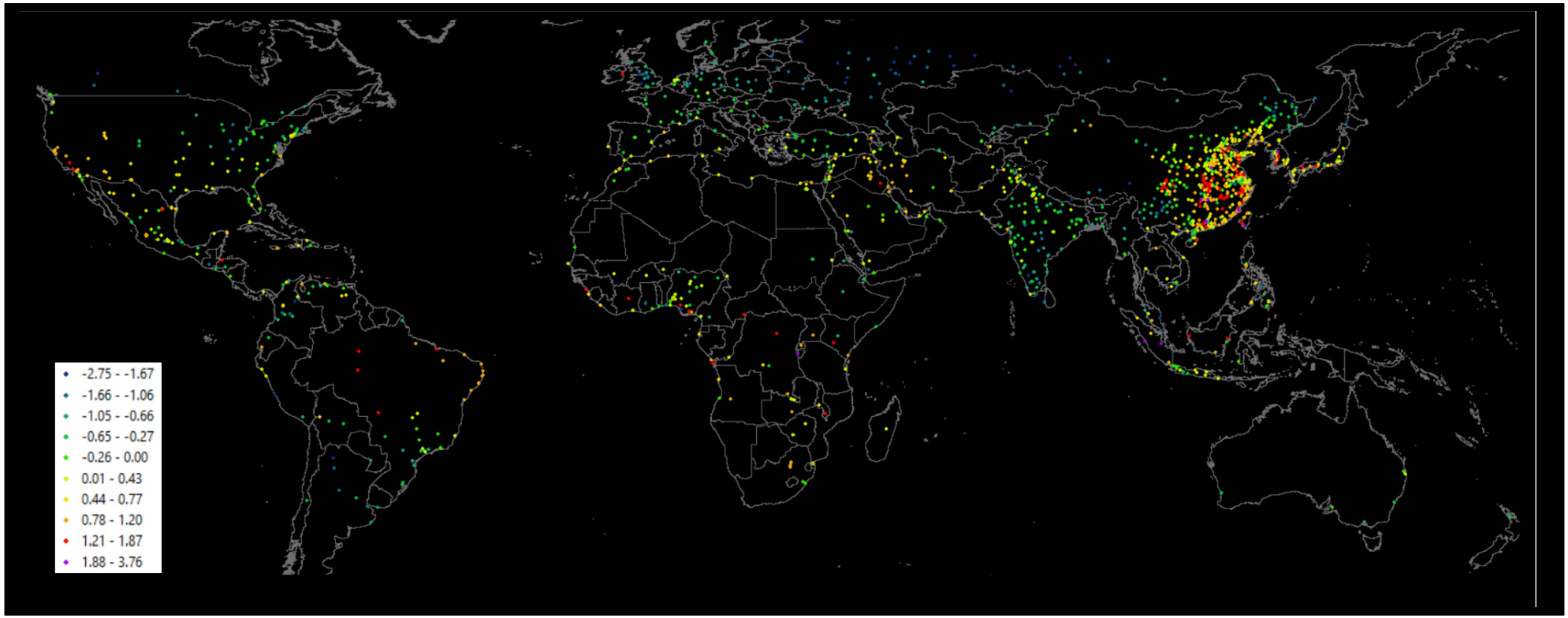

Figure 11: Distribution of city residuals by region*

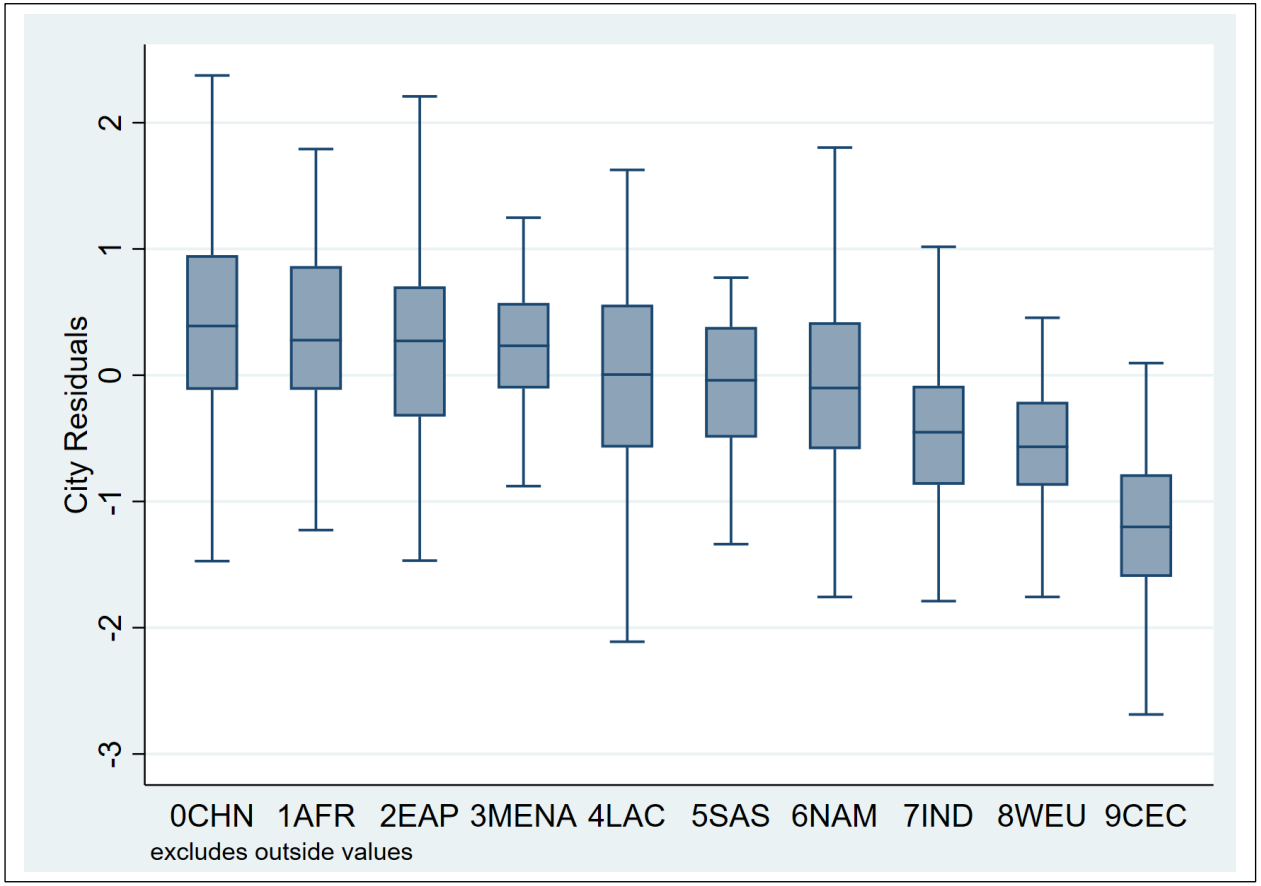

* CHN China; AFR Sub-Saharan Africa; EAP East Asia & Pacific (excluding China); MENA Middle East & North Africa
LAC Latin America & Caribbean; SAS South Asia (excluding India); NAM North America; IND India;
WEU Western Europe; CEC Former Comecon countries (Soviet Union, Eastern Europe)

Table 4: Mean decomposition share by region and source sector

Region	Cities	Region	Industry	Region	Fires
China	462	India	48.6	Sub-Saharan Africa	11.1
Former Comecon	67	Other East Asia & Pacific	44.5	Other East Asia & Pacific	2.3
India	91	China	42.4	Latin America & Caribbean	1.9
Latin America & Caribbean	159	Middle East & North Africa	35.0	Other South Asia	0.9
Middle East & North Africa	103	Other South Asia	32.8	India	0.7
North America	101	North America	22.0	Former Comecon	0.5
Other East Asia & Pacific	146	Sub-Saharan Africa	20.8	China	0.2
Other South Asia	22	Western Europe	20.8	Middle East & North Africa	0.1
Sub-Saharan Africa	92	Former Comecon	19.4	North America	0.1
Western Europe	91	Latin America & Caribbean	19.0	Western Europe	0.1

Region	Income	Region	Population	Region	Climate
Latin America & Caribbean	66.0	Sub-Saharan Africa	35.8	Former Comecon	54.9
North America	51.1	Other South Asia	22.5	China	29.2
Western Europe	49.8	India	17.0	Western Europe	27.4
Other East Asia & Pacific	35.7	Middle East & North Africa	9.6	North America	23.8
Middle East & North Africa	32.8	Latin America & Caribbean	9.0	Middle East & North Africa	22.6
Sub-Saharan Africa	32.0	Other East Asia & Pacific	7.0	Other South Asia	22.1
India	30.2	China	5.4	Other East Asia & Pacific	10.6
China	22.8	Former Comecon	3.6	Latin America & Caribbean	4.1
Other South Asia	21.7	North America	3.0	India	3.5
Former Comecon	21.5	Western Europe	2.0	Sub-Saharan Africa	0.3

Figure 12: CO2 Sources for a sample of cities
Global cities with populations > 500,000

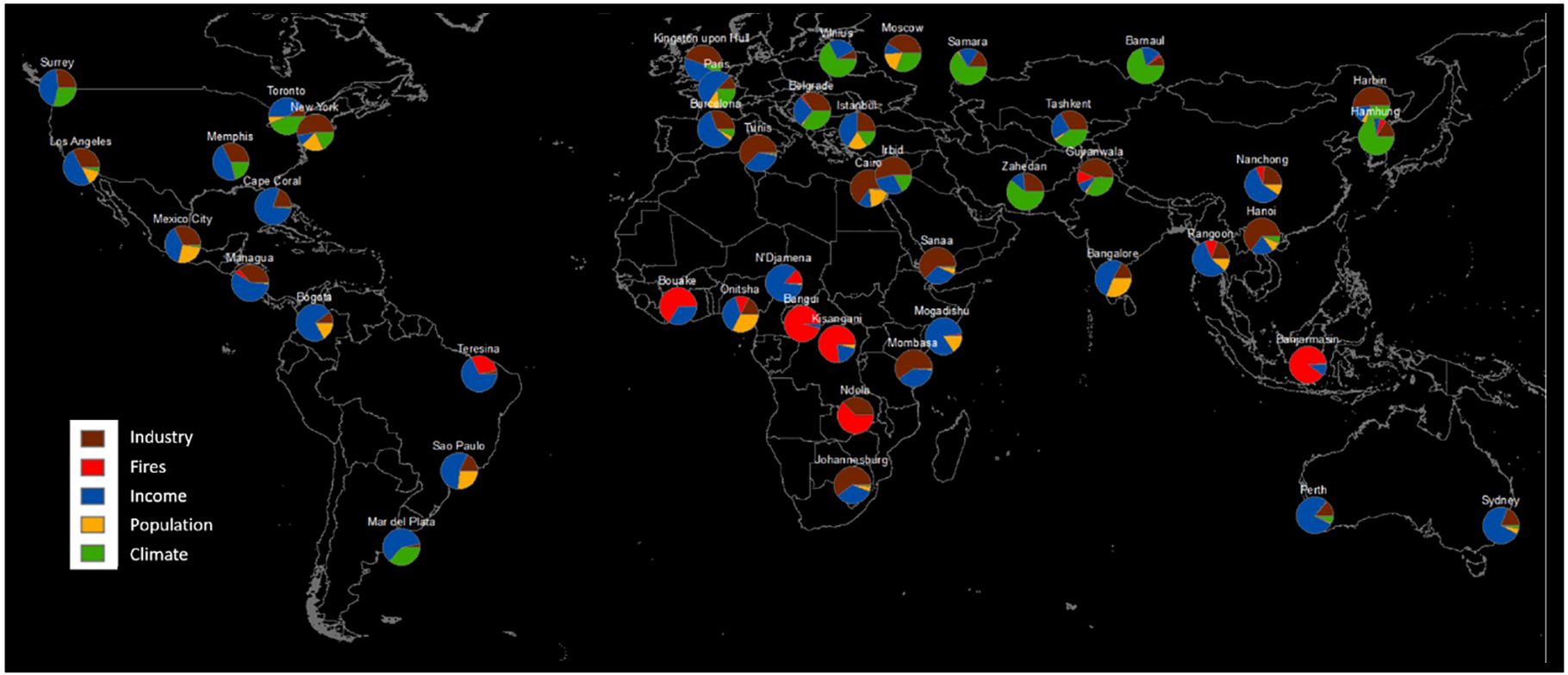

6.2 Implications for Non-Pigouvian Policies

Our results can also contribute to the discussion of strategies for achieving steep reductions in CO2 emissions. Most climate economists have argued for Pigouvian carbon pricing via emissions taxation or permit trading (Stiglitz and Stern 2021; Jacobs and van der Ploeg 2019; King et al. 2019; Klenert et al. 2018). Many policy analysts who support Pigouvian pricing also argue for a non-Pigouvian supplement: coordinated public investment in low-carbon land development, energy and transport that will accelerate the transition to low-carbon economies, particularly in lower-income countries that are not yet locked into high-carbon growth paths (van der Ploeg and Venables 2020). Economic growth is accompanied by urban development, which should avoid carbon-intensive land development, infrastructure and energy systems that are difficult to retrofit once they are locked in (Seto et al. 2014). The empirical literature suggests that lower-carbon residential, energy and transport development can have self-reinforcing effects on residents' preferences for low-carbon energy services (Carattini et al. 2018; Allcott and Rogers 2014) and transport modes (Weinberger and Goetzke 2010; Grinblatt et al. 2008; Bamberg et al. 2003).

While the non-Pigouvian argument is certainly plausible, the global resource implications of adopting it are huge and rigorous empirical support would be highly desirable. An attempt at rigorous testing would be premature for the current exercise, but an analysis of the residuals from our econometric model can provide suggestive evidence. Empirical leverage is provided by the diverse urban development paths followed by cities within and across countries. This is particularly true for investments in subway systems, undertaken by some cities but not by many others (Pasquale et al. 2016; Costa and Fernandes 2012; Jones 2008; Post 2007; Cudahy 1990). Subway installation has been motivated by the belief that it will shorten commuting times, reduce traffic congestion and vehicular emissions, and promote higher-density residential development near subway stations. Reduced vehicle emissions and energy efficiencies associated with higher-density development are frequently cited as carbon-saving advantages of mass transit systems.

From this perspective, subway cities should have had lower-carbon development paths, other things equal. We explore this proposition with our regression residuals, drawing on a recent global survey of subway systems by Turner and Gonzalez-Navarro (2018). Subways provide an excellent test of the non-Pigouvian supplement to carbon pricing for several reasons: They exemplify massive directed infrastructure investment; they are numerous but far from universal in most world regions; and their histories vary from over a century to less than a decade. If directed public investments can make a significant contribution to low-carbon development, the effect should register in a large sample that includes cities that have installed subway systems and cities that have not.

Our econometric results in Table 2 are very similar for all three urban radii, so we present the median case (40 km). We have residuals for 1,236 cities with populations greater than 500,000. The Turner/Gonzalez-Navarro survey identifies 132 of these as cities with subway systems. We divide the residuals into deciles, with the largest negative outliers in Decile 1. These are the cities whose measured CO2 concentrations are far lower than their predicted concentrations. In counterpoint, the cities in Decile 10 have measured concentrations far higher than their predictions. We count the number of cities with subways in each decile and present the results in Table 5. Figure 13 graphs the results with a regression line for easier interpretation. The results provide striking evidence of a negative relationship, with a decline of about 2 subway cities per decile. There are 23 subway cities

among the negative outliers in Decile 1, and only 6 subway cities among the positive outliers in Decile 10.

Table 5: Regression residuals: cities with subways by decile

Residual Decile	Cities	Subway Cities
1	123	23
2	124	19
3	123	19
4	124	16
5	124	13
6	123	11
7	124	9
8	123	7
9	124	9
10	124	6
Total	1,236	132

Figure 13: Cities with subways by residuals decile

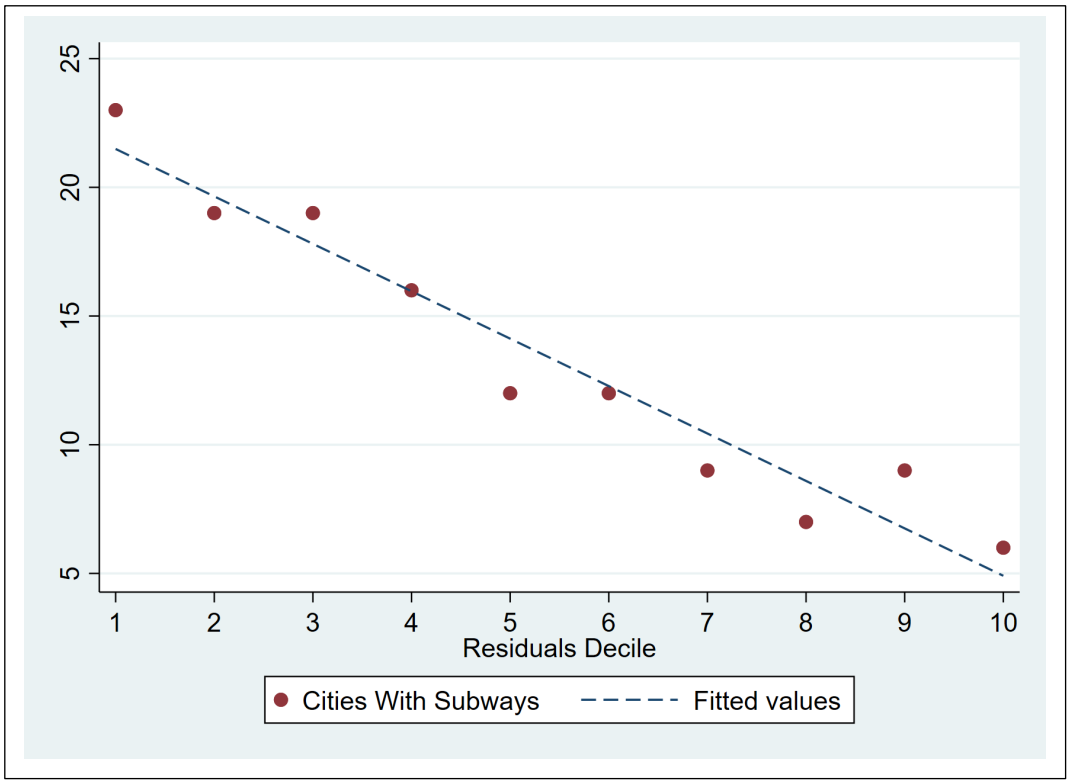

Our results certainly offer suggestive support for the view that large, directed public investments can make a significant contribution to low-carbon development. However, we cannot discount the potential role of endogeneity in this exercise. The implied relationship between mass transit investment and CO2 emissions has no explicit endogeneity, because reducing CO2 emissions has not been a goal of mass transit investments until very recently. However, traffic congestion has been a target, with local air pollution as a correlate. Some element of endogeneity may therefore be present, because CO2 emissions and local air pollutants have common sources in vehicle traffic, heavy industry, power generation, and residential heating. At the same time, the heterogeneity of global cities makes it unclear whether simultaneity is an important consideration in this case. Our database includes cities with and without subways in 138 countries, with some subway installations dating back more than a century, in political and economic regimes as varied as the former Soviet Union, other COMECON countries, social democratic regimes in Western Europe, military and populist authoritarian regimes in Latin America, relatively laissez-faire regimes in the United States and Australia, and regimes in Asia that range from authoritarian in the Democratic People's Republic of Korea and mainland China to relatively laissez-faire in Thailand and Taiwan, China. In light of these multiple, disparate factors, we believe that the exploratory results in Table 5 and Figure 13 offer reasonably strong evidence in favor of the public investment hypothesis. In future research, we hope to revisit this question in an econometric exercise with an explicit treatment of potential simultaneity.

7. Future Research[10]

The advent of satellite-based CO2 data has opened many research lines that could not be explored until the requisite information became available. In this section, we summarize some of the topics that have been identified in the course of our own research.

7.1 Quantifying CO2 Emissions

Although satellite-based measures of CO2 concentration anomalies are extremely useful for comparative analyses, the policy community would undoubtedly benefit from conversion of concentration anomalies to physical estimates of CO2 emissions. As we note in the paper, recent research for a few cities has used OCO-2 observations to produce scaling factors (R) for rough adjustment of ODIAC-type emissions estimates (Oda et al. 2018). Future extensions of our econometric work could include the construction of sectoral R-factors that could be used to improve emissions inventories by identifying the sources of their discrepancies from satellite-measured concentration anomalies. Hopefully, empirical research will ultimately depart from its continued dependence on emissions inventories by developing methods for direct conversion of satellite-measured CO2 anomalies to physical emissions estimates.

7.2 Potential Endogeneity Problems

[10] Our thinks to the reviewers of this paper for their useful thoughts about future research directions.

Two potentially-important problems with our current specification should be addressed in future work. The first relates to possible endogeneity in the relationship between CO2 emissions and mass transit investments. The second concerns joint determination of CO2 emissions and income per capita. Our results are consistent with the EKC hypothesis, but we recognize the need for more work on the problem. In a related vein, future research should explore the directions and sources of change in the emissions/income relationship. For example, the recent priority given to CO2 reduction in wealthier countries may already be changing the position or shape of the relationship at high income levels. Research on this issue should also investigate the intervening relationship between income and climate policies, which are now being registered in sources like the LSE's climate policy database (LSE/Grantham 2021).

7.3 Non-Pigouvian Policies

This paper has focused on subways because we have been able to use a large subway data set constructed by Turner and Gonzalez-Navarro (2018). However, we readily acknowledge that other mass transit systems may also have important effects on CO2 emissions (e.g., regional rail and bus rapid transit systems). As global data sets expand to include these systems, they should be incorporated into the analysis.

Explicit incorporation of mass transit investments into the econometric model will provide another avenue for future research. As previously noted, the possible joint determinacy of subway investments and CO2 emissions may warrant the use of instrumental variables in the expanded model. In addition, future research should investigate the contribution of subways and other mass transit investments to synergies between Pigouvian and non-Pigouvian policies. For example, a dynamic modeling exercise for the Paris urban area by Avner, Rentschler and Hallegatte (2014) suggests that the fuel price elasticity of carbon emissions can be much higher in cities with robust public transport options. An extension of the current econometric research would incorporate relevant price variables (e.g., fuel prices), as well as their interactions with transit investment variables to test the effects on price elasticities.

8. Summary and Conclusions

In this paper, we have estimated an urban CO2 emissions model using satellite-measured CO2 concentrations from 2014 to 2020, for 1,236 cities in 138 countries. The model incorporates the global trend in CO2 concentration, seasonal fluctuations by hemisphere, and a large set of georeferenced variables that incorporate CO2-intensive industry structure, emissions from agricultural and forest fires in neighboring areas, demography, the component of income that is uncorrelated with industry structure, and relevant geographic conditions. We resample all model variables to a 10 km global grid, and capture CO2 diffusion from discrete emissions sources via inverse-distance weighting to a grid cell centroid distance of 100 km.

In four econometric estimation exercises, we assign grid cells to cities if they lie within 20, 40 and 60 km of city centroids, or within the boundaries of UN-defined Functional Urban Areas. The results are very similar and robust in all four cases, with the expected signs and generally high levels of significance. We find that economic development has a significant effect on the direction of the

relationship between population density and CO2 emissions. The relationship is positive at very low incomes, but becomes negative at higher incomes. Our income results provide the first test of an Environmental Kuznets Curve relationship based on actual CO2 observations. With caveats about potential simultaneity problems, we find evidence for an EKC that reaches a peak in the range [$40,000 - $50,000] per capita, which is above the 90th percentile internationally.

We should note that our EKC results are only intended to provide a benchmark for judging future urban performance in reducing CO2 emissions. The same would be true if we had found a linear emissions/income relationship. We should also emphasize that our EKC results have no normative or policy implications in themselves. They do not imply that additional public resources are not needed for reducing CO2 emissions because "the problem will take care of itself" with continued economic growth. In fact, the opposite is true. Waiting for the EKC to reduce emissions from all countries would produce an enormous increase in cumulative CO2 and a potentially-catastrophic global temperature increase.

We explore other implications of our estimates in a series of exercises. Model-based predictions provide expected CO2 concentration anomalies for cities, given their sectoral, demographic, economic and geographic characteristics. We map the expected concentration anomalies and regression residuals for the 1,236 sample cities, using the residuals to index CO2 emissions performance that exceeds or falls short of model-based expectations. Among cities, we find wide variation in performance among cities within regions, as well as significant differences across regions. Overall city performance exceeds expectations in India, Western Europe and the former Comecon countries, while it falls short in China, the rest of East Asia & Pacific, Middle East & North Africa and Sub-Saharan Africa. We also decompose model CO2 predictions into five broad source categories for each city: Industry, Fires, Income (the component that is uncorrelated with Industry), Population and Climate. We find particularly important roles for Industry in India, China and other East Asia & Pacific countries; Fires in Sub-Saharan Africa; Income (the component uncorrelated with Industry) in Latin America & Caribbean, North America and Western Europe; Population in Sub-Saharan Africa, India and other South Asia countries; and Climate in the former Comecon countries.

Our results can also inform the discussion of policy instruments for CO2 emissions reduction. Many policy analysts who support Pigouvian pricing also argue for a non-Pigouvian supplement: coordinated public investment in low-carbon land development, energy and transport that will accelerate the transition to low-carbon economies. We explore this proposition for subway investments, drawing on a recent global survey of subway systems. We divide our 1,236 regression residuals into deciles, with the largest negative residuals in the first decile, and identify the subset of 132 global subway cities in each decile. We find that subway cities are four times more numerous among first-decile cities than among tenth-decile cities. We also find that representation of subway cities declines steadily across deciles. While these results provide strong suggestive support for the non-Pigouvian view, they are subject to potential endogeneity that should be explored in future research.

To conclude, this paper offers a response to the World Bank's new climate change mandate, which requires new metrics for judging progress in CO2 emissions reduction. We demonstrate that satellite-based CO2 measures can contribute by enabling rigorous analysis and performance assessment for all global cities and regions. We have estimated a CO2 emissions model for 1,236 cities with populations greater than 500,000, but our 10 km grid covers all terrestrial areas of the

globe. The same model could be used in other geographic domains, such as large and small cities within regions or countries, regions within countries, or specific project areas. In light of the World Bank's mandate for new metrics to track progress in greenhouse gas reduction, we hope to extend this pilot initiative to an open-source, regularly-updated CO2 database that will inform all global stakeholders.

Table A1: City CO2 results, top and bottom 15 residuals, China

Country	City	CO2	CO2_Predicted	CO2_Residual	Industry%	Fires%	Income%	Population%	Climate%
China	Shulan	400.556	403.28	-2.72	18.5	0	32	2.8	46.7
China	Qamdo	403.515	405.423	-1.91	0	0	11.2	1	87.9
China	Xiping	407.311	409.198	-1.89	30.8	0.1	10.6	1.6	56.9
China	Harbin	401.381	403.139	-1.76	50.3	0.3	13.5	7.5	28.4
China	Zhaotong	403.676	405.149	-1.47	2.7	0.2	15.5	17	64.6
China	Foshan	403.947	405.414	-1.47	62.2	0.4	27.9	6.4	3
China	Hegang	403.503	404.945	-1.44	15.5	0.1	11.7	1.9	70.8
China	Xuanzhou	408.48	409.908	-1.43	71.1	0	13.6	1.8	13.5
China	Rongcheng	402.877	404.254	-1.38	32	0.1	9.8	3.4	54.7
China	Wuhu	405.106	406.421	-1.31	82.8	0.1	7.5	1.7	7.9
China	Taihecun	405.507	406.752	-1.25	26	0.5	12.5	1.2	59.8
China	Beijing	403.994	405.227	-1.23	42.6	0.2	23.2	19.1	14.9
China	Qinzhou	402.828	404.036	-1.21	70.8	0.2	13.9	5.6	9.6
China	Hailun	404.325	405.53	-1.2	0.2	0.6	15	1.7	82.5
China	Yingkou	403.697	404.904	-1.21	43.6	0.1	24.6	2.6	29.1
China	Zhaoqing	407.384	405.751	1.63	63.2	0.4	20.6	10	5.8
China	Xiantao	406.765	405.107	1.66	39.9	0.5	26.4	2.4	30.8
China	Taishan	407.133	405.457	1.68	66	0.2	27.3	2.2	4.2
China	Zhongba	407.533	405.853	1.68	46.3	0.2	33.4	4	16.1
China	Jingling	407.182	405.463	1.72	39.7	0.4	20	4.2	35.8
China	Zhangshu	406.974	405.251	1.72	34.8	0.1	30.5	1.3	33.4
China	Chuzhou	406.705	404.954	1.75	65.6	0	21.2	4.8	8.4
China	Wutong	412.241	410.428	1.81	37	0	23.5	0.3	39.2
China	Mianyang	409.456	407.596	1.86	37.2	0.2	33.7	26.6	2.4
China	Anlu	403.241	401.371	1.87	29.3	0.1	20	2	48.6
China	Sihui	409.649	407.511	2.14	35	0.1	33.9	1	30
China	Fuqing	406.64	404.397	2.24	50.8	0	38.6	1.5	9.1
China	Jianshe	408.734	406.36	2.37	33.1	0	14	0.6	52.2
China	Lianyuan	407.585	404.918	2.67	67	0	28.4	4.6	0
China	Zhuzhou	404.562	400.799	3.76	40.2	0	18.4	4.2	37.2

Table A2: City CO2 results, top and bottom 15 residuals, East Asia & Pacific (excluding China)

Country	City	CO2	CO2_Predicted	CO2_Residual	Industry%	Fires%	Income%	Population%	Climate%
Indonesia	Patam	409.217	411.971	-2.75	81.1	0.4	16.8	1.8	0
Malaysia	Kuantan	409.781	411.841	-2.06	15.1	0	82.7	2.2	0
Japan	Sapporo	400.934	402.403	-1.47	12.3	0.2	67.3	4.9	15.3
Malaysia	Klang	403.12	404.45	-1.33	48.4	0	49.7	1.9	0
Philippines	Muntinlupa City	409.788	410.919	-1.13	63.6	0	36.4	0	0
Philippines	Cebu City	403.138	404.205	-1.07	65.9	0.1	34	0	0
Mongolia	Ulaanbaatar	403.622	404.676	-1.05	4.7	0	7.1	2.6	85.7
Philippines	San Jose del Monte	408.386	409.349	-0.96	80.9	0.3	16.8	2	0
Myanmar	Mandalay	403.21	404.121	-0.91	53.3	8.6	22	16.1	0
Vietnam	Hanoi	407.006	407.893	-0.89	58.5	0.3	19.2	16.7	5.3
Vietnam	Hai Duong	401.917	402.773	-0.86	86.6	0.1	12.5	0.8	0
Japan	Sagamihara	403.129	403.982	-0.85	45.5	0	53.1	1.4	0
Vietnam	Ho Chi Minh City	405.81	406.636	-0.83	40.3	0.9	15.7	43.2	0
Malaysia	Butterworth	406.493	407.309	-0.82	28	4.2	63.7	4	0
Korea, Dem. People’s Rep.	Ch'ongjin	404.455	405.2	-0.75	53.9	0	25.5	2	18.6
Philippines	Dasmarinas	406.767	405.78	0.99	66	0	32.2	1.8	0
Korea, Rep.	Jeonju	407.353	406.346	1.01	17.2	0	41.5	1.1	40.2
Korea, Dem. People’s Rep.	Pyongyang	405.689	404.644	1.05	43.8	0	2.8	11.8	41.6
Lao PDR	Vientiane	406.622	405.542	1.08	3.4	3.5	75.1	17.9	0
Japan	Kobe	405.061	403.852	1.21	59.4	0	31.7	0.8	8.1
Japan	Hiroshima	405.628	404.397	1.23	32	0.2	55.3	1.8	10.7
Korea, Rep.	Cheongju	406.278	405.006	1.27	39.3	0.1	29.3	0.5	30.7
Taiwan, China	Tainan	406.237	404.748	1.49	61.8	0	34.8	3.4	0
Korea, Rep.	Gwangju	407.532	406.014	1.52	21.2	0	38.8	2.2	37.8
Indonesia	Samarinda	405.265	403.623	1.64	2.9	3.6	86.7	6.7	0
Indonesia	Pontianak	407.145	405.472	1.67	0	9.2	77.3	13.4	0
Korea, Rep.	Yanggok	405.208	403.176	2.03	43.1	0.1	2.9	1.9	52
Taiwan, China	Pingtung	408.493	406.328	2.17	43.2	0	55.1	1.5	0.2
Indonesia	Jambi	407.93	405.721	2.21	0	1.3	90.7	8	0
Indonesia	Padang	405.221	402.487	2.73	78.2	0	17.8	4	0

Table A3: City CO2 results, top and bottom 15 residuals, Former Comecon Countries

Country	City	CO2	CO2_Predicted	CO2_Residual	Industry%	Fires%	Income%	Population%	Climate%
Russian Federation	Voronezh	402.071	404.758	-2.69	14	0.4	16.9	4.2	64.5
Russian Federation	Moscow	402.892	405.193	-2.3	37.4	0.1	9.1	25.4	28
Russian Federation	Kemerovo	400.798	403.004	-2.21	41.9	0.3	20.9	1.8	35.1
Russian Federation	Naberezhnyye Chelny	403.65	405.819	-2.17	20.1	0.1	16.7	1.5	61.7
Russian Federation	Kazan	401.291	403.448	-2.16	4.7	0.3	18.2	4.6	72.2
Russian Federation	Ulyanovsk	401.971	404.011	-2.04	21.2	0.5	17.5	2.1	58.7
Russian Federation	Yekaterinburg	403.193	405.231	-2.04	29.6	0.6	20.6	3.8	45.4
Russian Federation	Tyumen	402.94	404.971	-2.03	4.4	0	36.2	2	57.3
Russian Federation	Saint Petersburg	401.789	403.752	-1.96	35.8	0.3	18.9	15.9	29.2
Russian Federation	Samara	400.683	402.544	-1.86	15.5	0.4	18.5	2.6	63
Russian Federation	Kirov	402.584	404.435	-1.85	13.4	0	11.7	1.7	73.2
Russian Federation	Chelyabinsk	403.245	405.047	-1.8	35.6	1.3	12	2.3	48.8
Russian Federation	Tomsk	401.856	403.6	-1.74	13	0	26.7	2.4	57.8
Russian Federation	Lipetsk	402.26	404.001	-1.74	40.7	0.4	14.1	1.6	43.2
Kazakhstan	Qaraghandy	401.207	402.93	-1.72	38.6	0.8	27.1	1.1	32.5
Russian Federation	Irkutsk	404.205	404.965	-0.76	19.7	0.8	15.5	1.5	62.5
Ukraine	Kryvyy Rih	403.773	404.519	-0.75	39.3	0.7	9.3	2	48.6
Moldova	Chisinau	400.846	401.566	-0.72	11	0.3	9.3	2.6	76.6
Ukraine	Odesa	402.927	403.493	-0.57	23.2	0.9	13.5	4.7	57.7
Czech Republic	Prague	403.304	403.861	-0.56	27.3	0	41.9	1.9	29
Turkmenistan	Ashgabat	402.961	403.454	-0.49	18.4	0.1	52.2	6.4	22.9
Uzbekistan	Tashkent	404.312	404.77	-0.46	31.5	0.1	24.8	7.3	36.2
Russian Federation	Vladivostok	402.642	403.092	-0.45	11.1	0.4	16.2	1.6	70.8
Poland	Krakow	403.044	403.422	-0.38	32.2	0.6	28.4	1.5	37.3
Russian Federation	Penza	402.833	403.116	-0.28	1.8	0.3	9.7	2	86.2
Bulgaria	Sofia	404.006	404.228	-0.22	5.7	0.5	26	3.2	64.6
Hungary	Budapest	402.91	403.119	-0.21	16.1	0	46.1	4.1	33.7
Uzbekistan	Samarkand	404.936	404.947	-0.01	1.2	0.2	27	4.7	67
Russian Federation	Krasnodar	403.529	403.433	0.1	21.1	2.2	19.5	3.5	53.6
Tajikistan	Dushanbe	406.082	405.617	0.46	37.4	0	11.1	6.1	45.3

Table A4: City CO2 results, top and bottom 15 residuals, India

Country	City	CO2	CO2_Predicted	CO2_Residual	Industry%	Fires%	Income%	Population%	Climate%
India	Mysore	401.858	403.648	-1.79	41.4	0.3	45.5	12.7	0
India	Bezwada	403.359	404.719	-1.36	83.4	0.4	11	5.2	0
India	Coimbatore	402.459	403.775	-1.32	34.2	0	53.3	12.5	0
India	Indore	404.192	405.46	-1.27	13.9	0.3	39.1	46.8	0
India	Chanda	404.227	405.487	-1.26	93.4	0	5.6	1	0
India	Delhi	404.379	405.594	-1.21	26.9	0	8.8	63.5	0.8
India	Kolkata	405.52	406.701	-1.18	27.7	0	10.3	62	0
India	Hyderabad	403.29	404.4	-1.11	20.5	0.1	27.9	51.5	0
India	Trichinopoly	401.424	402.516	-1.09	84.2	0	12.1	3.7	0
India	Ahmadabad	403.447	404.498	-1.05	22	0	25.9	52.1	0
India	Amravati	403.41	404.448	-1.04	63.9	0.1	29.9	6.1	0
India	Tinnevelly	403.161	404.188	-1.03	81.1	0.1	16.1	2.7	0
India	Bangalore	404.118	405.13	-1.01	7.3	0.4	23.3	69	0
India	Gwalior	404.826	405.821	-1	19.1	0.3	39.5	31.9	9.3
India	Nagpur	403.679	404.652	-0.97	83.7	0.1	9.1	7.1	0
India	Bareilly	406.001	405.888	0.11	32	1.9	33.8	21.1	11.2
India	Jammu	406.704	406.577	0.13	3.9	0.2	29.8	6.4	59.7
India	Nanded	404.777	404.636	0.14	11.7	1.3	72.1	14.9	0
India	Hubli	405.402	405.206	0.2	21.1	0.2	59	19.7	0
India	Thiruvananthapuram	403.557	403.302	0.25	12.2	0.3	79.5	7.9	0
India	Saharanpur	407.181	406.879	0.3	31.4	0.4	35.1	6.6	26.5
India	Kota	405.35	405.044	0.31	75.7	0.7	15	8.3	0.3
India	Patna	405.053	404.688	0.37	50.6	0.1	16.9	31.3	1
India	Bhilai	406.48	406.091	0.39	87.4	0.3	8.8	3.5	0
India	Ghaziabad	403.689	403.295	0.39	72.6	0.2	10.6	16.6	0
India	Meerut	407.359	406.937	0.42	55.9	0.2	18.8	14.6	10.4
India	Ludhiana	405.98	405.548	0.43	47.1	6.4	23.5	11.5	11.4
India	Aligarh	408.265	407.735	0.53	56.7	0	22.1	16.5	4.7
India	Jalandhar	405.789	405.236	0.55	25.8	2.5	36	8	27.7
India	Bhavnagar	408.676	407.659	1.02	63.3	0	32	4.7	0

Table A5: City CO2 results, top and bottom 15 residuals, Latin America & the Caribbean

Country	City	CO2	CO2_Predicted	CO2_Residual	Industry%	Fires%	Income%	Population%	Climate%
Argentina	Salta	401.75	403.861	-2.11	13.2	0.7	43.8	3.1	39.1
Peru	Lima	400.334	402.265	-1.93	32.9	0	42.3	24.8	0
Colombia	Bucaramanga	402.612	404.319	-1.71	8.4	0.5	80.5	10.6	0
Colombia	Bogota	403.564	405.133	-1.57	5.5	0.4	43.1	50.9	0
Venezuela, RB	San Cristobal	407.595	409.028	-1.43	36.5	0.6	56.2	6.7	0
Brazil	Sao Jose dos Pinhais	400.664	402.059	-1.4	12.8	0.1	80.4	3.2	3.6
Argentina	Cordoba	401.807	403.188	-1.38	7.3	0.2	61.3	5.9	25.4
Argentina	San Miguel de Tucuman	402.074	403.403	-1.33	14.2	7.5	52	2.4	23.9
Argentina	Buenos Aires	402.297	403.552	-1.25	31.5	0.1	40	21.7	6.6
Guatemala	Guatemala City	404.016	405.191	-1.17	37.1	2.4	43.2	17.3	0
Colombia	Pereira	401.986	403.14	-1.15	13.5	0.6	80.4	5.5	0
Mexico	Xalapa	405.009	406.138	-1.13	22.7	1	60.8	4.5	11.1
Brazil	Santo Andre	402.715	403.831	-1.12	18.8	0.6	77.9	2.7	0
Brazil	Sao Paulo	404.738	405.706	-0.97	15.5	0	50.7	33.7	0
Brazil	Vila Velha	402.615	403.577	-0.96	0.1	9.1	80.2	10.6	0
Brazil	Joao Pessoa	404.136	403.246	0.89	26.1	3.2	69.7	1	0
Brazil	Fortaleza	404.421	403.5	0.92	25.8	1.1	61.3	11.9	0
Brazil	Salvador	406.089	405.167	0.92	33.2	0.1	52.9	13.8	0
Jamaica	Kingston	404.628	403.668	0.96	50.2	0.7	45.2	3.9	0
Brazil	Jaboatao	402.296	401.246	1.05	24.3	0.4	70.5	4.8	0
Brazil	Belem	405.766	404.706	1.06	6.6	1.4	65.6	26.4	0
Mexico	Zapopan	407.004	405.925	1.08	4	4.2	80.3	11.3	0.1
Brazil	Teresina	404.981	403.843	1.14	3	25.7	60.9	10.4	0
Ecuador	Guayaquil	404.224	403.074	1.15	21.7	1.3	58.4	18.6	0
Mexico	Guadalupe	405.268	404.046	1.22	25.1	0.7	63.1	3.2	8
Brazil	Cuiaba	403.263	402	1.26	8.9	0.7	87.6	2.8	0
Brazil	Manaus	404.834	403.52	1.31	14.7	0.6	76.3	8.4	0
Brazil	Sao Luis	402.829	401.357	1.47	31	0.4	52.3	16.3	0
Brazil	Natal	404.83	403.279	1.55	0.1	11.2	69.8	19	0
Honduras	San Pedro Sula	405.651	404.025	1.63	32.1	4.6	50.2	13.2	0

Table A6: City CO2 results, top and bottom 15 residuals, Middle East & North Africa

Country	City	CO2	CO2_Predicted	CO2_Residual	Industry%	Fires%	Income%	Population%	Climate%
Yemen, Rep.	Ta`izz	404.519	405.741	-1.22	52.1	0	25.3	22.6	0
Turkey	Trabzon	402.871	403.75	-0.88	5.5	0	87.8	6.7	0
Saudi Arabia	At Ta'if	403.871	404.702	-0.83	23.7	0	73.3	2.6	0.4
Turkey	Mersin	403.863	404.648	-0.79	23	0	38	4.8	34.2
Sudan	Khartoum North	403.19	403.823	-0.63	15	0	74	11	0
Turkey	Bursa	403.717	404.327	-0.61	19.2	0	46.2	5.8	28.8
Morocco	Meknes	404.612	405.201	-0.59	28.3	0	29.5	3.5	38.7
Sudan	Omdurman	403.419	403.994	-0.58	12.7	0	61.2	26.1	0
Sudan	Khartoum	404.523	405.081	-0.56	13	0	43.7	43.3	0
Turkey	Ankara	405.73	406.283	-0.55	15.8	0	36.1	11.5	36.6
Turkey	Eskisehir	403.859	404.365	-0.51	12.3	0	42.3	2.3	43
Turkey	Istanbul	404.82	405.248	-0.43	22.3	0	39.2	24.2	14.3
Turkey	Kayseri	403.073	403.452	-0.38	3.3	0	30.2	5.1	61.4
Egypt, Arab Rep.	Madinat as Sadis min Uktubar	402.389	402.737	-0.35	92.6	0	2.4	2.5	2.6
Turkey	Adana	404.459	404.769	-0.31	37.8	0.5	36.6	6	19.2
United Arab Emirates	Sharjah	405.231	404.457	0.77	76.7	0	18.6	4.7	0
Iran, Islamic Rep.	Esfahan	404.733	403.946	0.79	44.1	0	4.5	6.2	45.2
Iran, Islamic Rep.	Ahvaz	403.391	402.599	0.79	52.1	0.4	9.9	14.8	22.8
Armenia	Yerevan	404.676	403.881	0.8	14.8	0.1	18	4.6	62.5
Iran, Islamic Rep.	Qom	405.009	404.178	0.83	18	0	2.4	6.5	73.2
Morocco	Sale	406.084	405.245	0.84	21.1	0	48.5	5.4	25
Egypt, Arab Rep.	Port Said	406.746	405.904	0.84	48.7	0.1	20.4	19.3	11.6
Iraq	An Najaf	405.265	404.396	0.87	30.8	0	42.4	4.8	22
Iran, Islamic Rep.	Kermanshah	405.547	404.663	0.88	35	0.1	2.9	5.2	56.8
Iraq	Al Hillah	405.349	404.362	0.99	39.1	0	21.8	4.4	34.6
Kuwait	Kuwait City	404.642	403.646	1	72	0	19.8	5.8	2.4
Iraq	Baghdad	405.21	404.211	1	34.2	0	19.8	28.7	17.3
Iraq	Mosul	404.906	403.809	1.1	38	0.2	19.3	7.4	35.2
Iraq	Al Basrah	405.641	404.47	1.17	63.9	0.1	25.5	10.1	0.4
Iraq	An Nasiriyah	405.694	404.446	1.25	0.5	0.1	61.2	7.6	30.6

Table A7: City CO2 results, top and bottom 15 residuals, North America

Country	City	CO2	CO2_Predicted	CO2_Residual	Industry%	Fires%	Income%	Population%	Climate%
Canada	Edmonton	401.274	403.03	-1.76	20.5	0	43.4	1.5	34.5
Canada	Brampton	408.966	410.51	-1.54	7.3	0	49.6	1.1	42
Canada	Calgary	403.423	404.892	-1.47	5.5	0	51.7	2.2	40.6
United States	Indianapolis	402.515	403.968	-1.45	8.6	0	63.5	3.1	24.7
United States	Louisville	401.953	403.407	-1.45	38	0	44.7	1.3	15.9
United States	Baltimore	403.929	405.107	-1.18	42.1	0	48.6	3.5	5.8
United States	Grand Rapids	403.882	405.012	-1.13	14.1	0.1	65.9	1.3	18.6
Canada	Winnipeg	405.968	407.082	-1.11	0.4	0.1	41.4	1	57
United States	Providence	401.877	402.987	-1.11	20.5	0.1	39.9	1.6	37.9
United States	St. Louis	405.674	406.575	-0.9	36.4	0	40.5	2.6	20.5
United States	Rochester	402.94	403.837	-0.9	5.6	0	51.3	1.1	42
United States	Minneapolis	403.431	404.303	-0.87	15.5	0.1	39	3.5	41.9
United States	Columbus	402.556	403.369	-0.81	5	0	66	3.5	25.5
United States	Allentown	402.969	403.757	-0.79	32.3	0.2	35.9	0.8	30.8
United States	Detroit	405.081	405.776	-0.69	36	0	32.2	3.2	28.5
United States	Provo	403.88	403.261	0.62	11.6	0	52.5	0.8	35
United States	Ogden	404.48	403.853	0.63	3.5	0	58.1	1.2	37.3
United States	Hempstead	402.663	401.97	0.69	30.4	0	37.6	0	32
United States	Concord	405.39	404.673	0.72	27.2	0.1	59.8	0.6	12.3
United States	Virginia Beach	405.193	404.344	0.85	6	0	68	3.2	22.7
United States	Mesa	405.652	404.775	0.88	13	0	76.7	1.3	9
United States	San Francisco	406.174	405.29	0.88	26.5	0	62.8	6.5	4.2
United States	Sacramento	405.666	404.769	0.9	14.4	0.2	73.5	4.8	7.1
United States	Riverside	405.154	404.207	0.95	29.4	0.2	60.5	3	6.9
United States	Fresno	405.074	404.084	0.99	2.8	0.2	80.4	2	14.7
United States	Honolulu	405.739	404.667	1.07	22.4	0	77.4	0.2	0
United States	Mission Viejo	405.22	404.104	1.12	27.2	0.4	66.4	0	6
United States	San Jose	405.629	404.438	1.19	28.1	0	65	4.6	2.4
United States	Los Angeles	405.856	404.318	1.54	30.6	0.5	48.5	17	3.4
United States	Bakersfield	404.891	403.088	1.8	17	0.1	70	1.2	11.7

Table A8: City CO2 results, top and bottom 15 residuals, South Asia (excluding India)

Country	City	CO2	CO2_Predicted	CO2_Residual	Industry%	Fires%	Income%	Population%	Climate%
Nepal	Kathmandu	400.294	402.544	-2.25	5.1	0.1	47.2	0.2	47.5
Sri Lanka	Colombo	404.602	405.941	-1.34	52.6	0	47.4	0	0
Bangladesh	Khulna	402.286	403.075	-0.79	36.4	0.7	32.8	30	0
Bangladesh	Dhaka	403.924	404.518	-0.59	41.5	0	8.5	50	0
Bangladesh	Chattogram	404.823	405.325	-0.5	34.9	0.4	31.4	33.3	0
Pakistan	New Mirpur	405.325	405.812	-0.49	42.3	1.6	17.1	4.9	34.1
Pakistan	Saidu Sharif	403.427	403.867	-0.44	9.1	0	9.8	13.5	67.6
Pakistan	Islamabad	403.865	404.304	-0.44	65.5	0	7.7	6.2	20.6
Pakistan	Faisalabad	405.107	405.262	-0.15	23.7	0.4	30.9	37.8	7.2
Pakistan	Rawalpindi	404.443	404.561	-0.12	69.3	0	8.7	8.3	13.6
Pakistan	Karachi	405.054	405.017	0.04	55.8	0	12.2	31.9	0
Pakistan	Sargodha	405.043	404.871	0.17	53.2	0.5	28.6	7.9	9.7
Afghanistan	Kabul	404.21	403.959	0.25	0.4	0	4.6	16.9	78.1
Pakistan	Lahore	406.619	406.368	0.25	21	3.4	12.3	56	7.3
Pakistan	Bahawalpur	404.446	404.155	0.29	6.2	0.5	59.8	22	11.4
Pakistan	New Mirpur	405.325	405.812	-0.49	42.3	1.6	17.1	4.9	34.1
Pakistan	Saidu Sharif	403.427	403.867	-0.44	9.1	0	9.8	13.5	67.6
Pakistan	Islamabad	403.865	404.304	-0.44	65.5	0	7.7	6.2	20.6
Pakistan	Faisalabad	405.107	405.262	-0.15	23.7	0.4	30.9	37.8	7.2
Pakistan	Rawalpindi	404.443	404.561	-0.12	69.3	0	8.7	8.3	13.6
Pakistan	Karachi	405.054	405.017	0.04	55.8	0	12.2	31.9	0
Pakistan	Sargodha	405.043	404.871	0.17	53.2	0.5	28.6	7.9	9.7
Afghanistan	Kabul	404.21	403.959	0.25	0.4	0	4.6	16.9	78.1
Pakistan	Lahore	406.619	406.368	0.25	21	3.4	12.3	56	7.3
Pakistan	Bahawalpur	404.446	404.155	0.29	6.2	0.5	59.8	22	11.4
Pakistan	Quetta	404.548	404.075	0.47	2.2	0	12.7	12.7	72.4
Pakistan	Multan	404.513	404.022	0.49	34.2	0.7	32.3	25.8	6.9
Pakistan	Sialkot City	405.225	404.733	0.49	25.7	1.6	12.1	43.5	17.1
Pakistan	Peshawar	404.224	403.576	0.65	45.6	0	11	18.8	24.5
Pakistan	Gujranwala	407.156	406.384	0.77	31.4	8.1	6.9	30.3	23.3

Table A9: City CO2 results, top and bottom 15 residuals, Sub-Saharan Africa

Country	City	CO2	CO2_Predicted	CO2_Residual	Industry%	Fires%	Income%	Population%	Climate%
Nigeria	Warri	401.452	403.977	-2.52	31.2	15.3	34.7	18.8	0
Ghana	Kumasi	403.325	404.552	-1.23	0	1.7	61.1	37.1	0
Benin	Cotonou	403.496	404.64	-1.14	72.7	0.1	18.1	9.1	0
Cameroon	Yaounde	396.979	398.012	-1.03	0	0.4	56.1	43.4	0
Eritrea	Asmara	402.043	402.925	-0.88	15.4	0	34.6	50	0
Ethiopia	Addis Ababa	404.425	405.214	-0.79	41.1	0.6	17	41.3	0
Nigeria	Kano	402.197	402.747	-0.55	0	0.7	18.1	81.2	0
Nigeria	Maiduguri	402.068	402.567	-0.5	0	30	24.3	45.7	0
Nigeria	Sokoto	402.701	403.157	-0.46	56.7	0.3	14	29.1	0
Congo, Dem. Rep.	Mbuji-Mayi	396.933	397.324	-0.39	0	16.6	1	82.4	0
Kenya	Meru	402.768	403.149	-0.38	0.1	0.3	49.1	50.6	0
Nigeria	Abuja	404.341	404.719	-0.38	0	7.9	42.6	49.5	0
Togo	Lome	400.306	400.676	-0.37	44.6	0.9	33.3	21.2	0
Djibouti	Djibouti	404.991	405.356	-0.37	7.7	0	80.4	12	0
Nigeria	Enugu	406.115	406.478	-0.36	80.6	3.8	7.4	8.2	0
Nigeria	Ibadan	402.103	401.051	1.05	37.6	7	14.5	40.9	0
Kenya	Mombasa	403.213	402.16	1.05	50.1	0.7	33.8	15.4	0
Congo, Dem. Rep.	Lubumbashi	403.219	402.165	1.05	0.1	79.7	0.2	20	0
South Africa	Vereeniging	405.055	403.968	1.09	60.6	0.2	30.8	3.5	4.9
Angola	Huambo	406.121	404.965	1.16	1.4	0	78.2	20.4	0
Congo, Dem. Rep.	Kisangani	404.372	403.15	1.22	0	8.8	2.4	88.8	0
Guinea	Conakry	404.388	403.165	1.22	3.1	11.8	32	53	0
Nigeria	Benin City	398.832	397.596	1.24	31.5	0	25	43.4	0
Central African Republic	Bangui	403.819	402.484	1.34	0.4	89.8	3.9	5.9	0
Côte d'Ivoire	Bouake	405.226	403.852	1.37	0	60.4	30.7	8.9	0
Malawi	Blantyre	404.033	402.648	1.38	0.9	4.7	18.3	76.2	0
Nigeria	Aba	401.414	400.013	1.4	55	0	32.6	12.3	0
Angola	Cabinda	402.997	401.291	1.71	1.6	0	94.6	3.8	0
Kenya	Nairobi	403.964	402.172	1.79	12.6	0.3	24.1	63	0
Burundi	Bujumbura	405.087	402.727	2.36	9.3	0	20.1	70.6	0

Table A10: City CO2 results, top and bottom 15 residuals, Western Europe

Country	City	CO2	CO2_Predicted	CO2_Residual	Industry%	Fires%	Income%	Population%	Climate%
United Kingdom	Leicester	403.948	405.836	-1.89	14.7	0	48.4	0	36.9
United Kingdom	Sheffield	403.063	404.819	-1.76	44.9	0	30.1	0.5	24.4
United Kingdom	Liverpool	401.752	403.502	-1.75	15.3	0	50.6	1	33.1
United Kingdom	Bristol	404.729	406.446	-1.72	19.5	0	54	0.2	26.2
United Kingdom	Nottingham	403.123	404.664	-1.54	47.7	0	30	0.7	21.6
Sweden	Stockholm	400.801	402.333	-1.53	4.8	0	73.9	3.1	18.2
Germany	Essen	406.455	407.911	-1.46	56.9	0	24.3	0.5	18.4
Lithuania	Vilnius	400.302	401.541	-1.24	7.3	0.1	25.8	1.9	65
United Kingdom	Manchester	403.882	405.114	-1.23	18.1	0	48	3.6	30.2
Latvia	Riga	402.151	403.383	-1.23	4.4	0	36.6	1.2	57.8
United Kingdom	Birstall	404.298	405.488	-1.19	29.6	0	38.7	1.9	29.8
Germany	Dortmund	404.689	405.752	-1.06	51.8	0	27.9	0.1	20.3
Germany	Cologne	403.488	404.464	-0.98	59.8	0	29.4	0.4	10.3
United Kingdom	London	404.351	405.274	-0.92	7.9	0	48.8	15.1	28.2
United Kingdom	Kingston upon Hull	407.151	408.068	-0.92	44.2	0.1	44.8	0.6	10.4
Germany	Stuttgart	405.707	405.732	-0.03	22.3	0	45.5	0.4	31.8
Germany	Frankfurt	405.261	405.282	-0.02	24.7	0	49.7	0.2	25.4
Spain	Valencia	404.661	404.601	0.06	16.5	0.2	79.1	0	4.2
Netherlands	Amsterdam	405.657	405.595	0.06	30.5	0.2	45	0.4	24
Italy	Genoa	403.918	403.747	0.17	12.1	0	65.7	0.4	21.9
Germany	Nuremberg	403.274	402.994	0.28	5.7	0	53.7	1	39.6
Greece	Athens	405.426	405.129	0.3	18.1	0	59.9	0	22
Italy	Palermo	404.721	404.422	0.3	13.3	0.8	84.5	1.4	0
Netherlands	The Hague	405.297	404.956	0.34	35.7	0.2	62.4	0.5	1.2
France	Marseille	403.574	403.215	0.36	27.2	0.2	67.5	0.7	4.5
Netherlands	Rotterdam	405.605	405.243	0.36	28.5	0	59.6	1.7	10.1
Spain	Malaga	404.417	404.034	0.38	9.6	0	65.6	1.1	23.7
Portugal	Lisbon	404.412	404.007	0.4	14.8	0.1	59.1	0	25.9
Spain	Barcelona	405.573	405.118	0.45	29.9	0	59.6	3.9	6.6
Ireland	Dublin	409.363	407.877	1.49	86.6	0	0	13.4	0

References

Allcott, H. and T. Rogers. 2014. The short-run and long-run effects of behavioral interventions: experimental evidence from energy conservation, American Economic Review, 104(10): 3003-37.

Apergis, N., Payne, J.E. 2014. Renewable energy, output, CO2 emissions, and fossil fuel prices in Central America: Evidence from a non linear panel smooth transition vector error correction model. Energy Economics 42: 226–232.

Auch, T. 2017. Tracking Oil Refineries and Their Emissions: a complete inventory of global oil refineries. https://www.fractracker.org/2017/12/global-oil-refineries-emissions/

Avner, P., J. Rentschler and S. Hallegatte. 2014. Carbon Price Efficiency Lock-in and Path Dependence in Urban Forms and Transport Infrastructure. World Bank Policy Research Working Paper No. 2941.

Bamberg, S., D. Rölle and C. Weber. 2003. Does habitual car use not lead to more resistance to change of travel mode?, Transportation, 30(1): 97-108.

Ben Youssef, A., S. Hammoudeh and A. Omri. 2016. Simultaneity Modeling Analysis of the Environmental Kuznets Curve. Energy Economics, 60: 266-274.

Byers, L., J. Friedrich et al. 2021. A Global Database of Power Plants. World Resources Institute.

C40 (2021). C40 Greenhouse Gas Emissions Dashboard Data, March.

Carattini, S., M. Péclat and A. Baranzini. 2018. Social interactions and the adoption of solar PV: evidence from cultural borders, Policy Working Paper No. 339, LSE Centre for Climate Change Economics.

CIESIN (Center for International Earth Science Information Network, Columbia University). 2018. Documentation for the Gridded Population of the World, Version 4 (GPWv4), Revision 11.

Costa, A. and R. Fernandes. 2012. Urban public transport in Europe: Technology diffusion and market organization. Transportation Research Part A: Policy and Practice, 46(2): 269-284.

Csereklyei, Z. and D. Stern. 2015. Global energy use: decoupling or convergence? Energy Econ. 51, 633–641.

Cudahy, Brian. 1990. Cash, Tokens, and Transfers: A History of Urban Mass Transit in North America. New York: Fordham University Press.

Dasgupta, S., B. Laplante, H. Wang and D. Wheeler. 2002. Confronting the Environmental Kuznets Curve. Journal of Economic Perspectives, 16(1): 147–168.

Dasgupta, S., S. Lall and D. Wheeler. 2021. Traffic, Air Pollution and Distributional Impacts in Dar es Salaam: A Spatial analysis with New Satellite Data, Science of the Total Environment (forthcoming).

EOG (Earth Observation Group). 2021. VIIRS Global Nighttime Lights. NASA Repository, Payne Institute of Public Policy, Colorado School of Mines.

Gale, J. et al. 2005. Chapter 2: Sources of CO2, in Metz, B., D. Ogunlade et al., Carbon Dioxide Capture and Storage. Cambridge University Press, UK.

GEM (Global Energy Monitor). 2021. Global Steel Plant Tracker.

Gasser, T., L. Crepin, Y. Quilcaille, R. Houghton, P. Ciais and M. Obersteiner. 2020. Historical CO2 emissions from land use and land cover change and their uncertainty. Biogeosciences, 17: 4075–4101.

Grinblatt, M., M. Keloharju and S. Ikäheimo. 2008. Social influence and consumption: evidence from the automobile purchases of neighbors, The Review of Economics and Statistics, 90(4): 735-753.

Heger M., D. Wheeler, G. Zensa and C. Meisner. 2018. Motor Vehicle Density and Ambient Air Pollution in Greater Cairo – How Did Fuel Subsidy Removal and Metro Line Extension Effect Congestion and Pollution? Washington DC: World Bank.

IPCC. 2018. Chapter 2 (Rogelj, J., D. Shindell, K. Jiang, et al.): Mitigation Pathways Compatible with 1.5°C in the Context of Sustainable Development. In: Global Warming of 1.5°C. An IPCC Special Report.

IPCC. 2021. Climate Change 2021: The Physical Science Basis

Jacobs, B. and F. van der Ploeg. 2019. Redistribution and pollution taxes with nonlinear Engel curves, Journal of Environmental Economics and Management, 95: 198-226.

Jones, D. 2008. Mass Motorization + Mass Transit: An American History and Policy Analysis. Bloomington: Indiana University Press.

Jotzo, F., P. Burke, P. Wood, A. Macintosh and D. Stern. 2012. Decomposing the 2010 global carbon dioxide emissions rebound. Nat. Clim. Chang. 2(4): 213–214.

JPL/NASA. 2021. OCO-2 Data Set. Jet Propulsion Laboratory, California Institute of Technology. https://co2.jpl.nasa.gov/?mission=oco-2

Keeling, C., et al. 1976. Atmospheric carbon dioxide variations at Mauna Loa Observatory, Hawaii. Tellus, 28(6): 538-551.

King, M., B. Tarbush and A. Teytelboym. 2019. Target carbon tax reforms, European Economic Review, 119.

Klenert, D., L. Mattauch, E. Combet, O. Edenhofer, C. Hepburn, R. Rafaty and N. Stern. 2018. Making carbon pricing work for citizens, Nature Climate Change, 8: 669-677.

Labzovskii, L., S. Jeong and N. Parazoo N. 2019. Working towards confident spaceborne monitoring of carbon emissions from cities using Orbiting Carbon Observatory-2. Remote Sens. Environ. 233: 111359.

Lawell, C. and Z. Liscow. 2013. Endogeneity in the Environmental Kuznets Curve: An Instrumental Variables Approach. American Journal of Agricultural Economics, 95: 268-274.

LSE/Grantham Research Institute on Climate Change and the Environment. 2021. Climate Change Laws of the World.

McCaffrey, R. et al. 2021. Global Cement Directory. Pro Global Media Limited, Octagon House, Surrey, United Kingdom.

Mistry, M. 2019. Historical global gridded degree days: A high spatial resolution database of CDD and HDD. Geoscience Data Journal, 6(2): 214-221.

Nordhaus, W., A. Azam et al. 2006. The G-Econ Database on Gridded Output: Methods and Data. Yale University.

Oda, T., S. Maksyutov and R. Andres. 2018 The open-source data inventory for anthropogenic CO2, version 2016 (ODIAC2016): a global monthly fossil fuelCO2 gridded emissions data product for tracer transport simulations and surface flux inversions. Earth Syst. Sci. Data, 10: 87–107.

Pan, G., X. Yuan and M. Jieqi. 2021. The potential of CO2 satellite monitoring for climate governance: A review. Journal of Environmental Management, 277: 111423.

Pasquale, G., A. Santos, A. Leal and M. Tozzi. 2016. Innovative Public Transport in Europe, Asia and Latin America: A Survey of Recent Implementations. Transportation Research Procedia, 14: 3284-3293.

Post, R. 2007. Urban Mass Transit: The Life Story of a Technology. Westport, CT: Greenwood.

Raupach, M., G. Marland, P. Ciais, C. Le Quéré, et al. 2007. Global and regional drivers of accelerating CO2 emissions. Proc. Natl. Acad. Sci. 104(24): 10288–10293.

Reuters. 2018. Global temperatures on track for 3-5 degree rise by 2100: U.N. https://www.reuters.com/article/us-climate-change-un/global-temperatures-on-track-for-3-5-degree-rise-by-2100-u-n-idUKKCN1NY186?edition-redirect=uk

Sanchez, L. and D. Stern. 2016. Drivers of industrial and non-industrial greenhouse gas emissions. Ecological Economics, 124:17–24.

Schiavina, M., A. Moreno-Monroy, L. Maffenini and P. Veneri, Paolo. 2019. GHS-FUA R2019A - GHS functional urban areas, derived from GHS-UCDB R2019A (2015). European Commission, Joint Research Centre (JRC) [Dataset] doi:10.2905/347F0337-F2DA-4592-87B3-E25975EC2C95 PID: http://data.europa.eu/89h/347f0337-f2da-4592-87b3-e25975ec2c95.

Seto, K., S. Dhakal et al. 2014. Human settlements, infrastructure and spatial planning, in Climate Change 2014: Mitigation of Climate Change, Contribution of Working Group III to the Fifth Assessment Report of the Intergovernmental Panel on Climate Change.

Steffen, W., J. Rockström and K. Richardson. 2018. Trajectories of the Earth System in the Anthropocene. PNAS 115(33): 8252-8259.

Stiglitz, J. and N. Stern. 2021. The Social Cost of Carbon, Risk, Distribution, Market Failures: An Alternative Approach. National Bureau of Economic Research Working Paper No. 28472.

Thoning, K. et al. 1989. Atmospheric carbon dioxide at Mauna Loa Observatory: 2. Analysis of the NOAA GMCC data, 1974–1985. Journal of Geophysical Research: Atmospheres. 94(D6): 8549-8565.

Turner, M. and M. Gonzalez-Navarro. 2018. Subways and urban growth: Evidence from earth. Journal of Urban Economics 108: 85-106.

Van Ewijk, C. and S. van Wijnbergen. 1995. Can abatement overcome the conflict between environment and economic growth? De Economist, 143: 197–216.

Van der Ploeg, R. and A. Venables. 2020. Proposals for Effective Climate Policies: Climate Complementarities and Flywheel Effects. University of Oxford, February.

Van der Werf, G. , J. Randerson et al. 2017. Global fire emissions during 1997-2016. Earth Syst. Sci. Data, 9: 697–720.

Weinberger, R. and F. Goetzke. 2010. Unpacking preference: how previous experience affects auto ownership in the United States, Urban Studies, 47(10):2111-2128.

Winkler, K., R. Fuchs, M. Rounsevell et al. 2021. Global land use changes are four times greater than previously estimated. Nature Communications, 12: 2501.

World Bank. 2012. Turn Down the Heat ~ Why a 4°C warmer world must be avoided. World Bank: Washington, D.C.

World Bank. 2021. World Bank Group President's Statement on Climate Change Action Plan. https://www.worldbank.org/en/news/statement/2021/04/02/world-bank-group-president-statement-on-climate-change-action-plan

World Cities Database. 2021. https://simplemaps.com/data/world-cities

Wu, D., J. Lin, T. Oda and E. Kort. 2020. Space-based quantification of per capita CO2 emissions from cities. Environmental Research Letters, 15: 035004.

Ye, X., T. Lauvaux, E. Kort, T. Oda, S. Feng, J. Lin, E. Yang and D. Wu. 2020. Constraining fossil fuel CO2 emissions from urban area using OCO-2 observations of total column CO2. JGR Atmospheres, 125(8).